European Journal of Medicinal Chemistry 183 (2019) 111677

Contents lists available at ScienceDirect

European Journal of Medicinal Chemistry

journal homepage: http://www.elsevier.com/locate/ejmech

Research paper

Synthesis of benzotriazoles derivatives and their dual potential as α-amylase and α-glucosidase inhibitors *in vitro*: Structure-activity relationship, molecular docking, and kinetic studies

Shehryar Hameed [a], Kanwal [a], Faiza Seraj [a], Rafaila Rafique [a], Sridevi Chigurupati [b], Abdul Wadood [c], Ashfaq Ur Rehman [c], Vijayan Venugopal [d], Uzma Salar [e], Muhammad Taha [f], Khalid Mohammed Khan [a, f, *]

[a] H. E. J. Research Institute of Chemistry, International Center for Chemical and Biological Sciences, University of Karachi, Karachi, 75270, Pakistan
[b] Department of Medicinal Chemistry and Pharmacognosy, College of Pharmacy, Qassim University, Buraidah, 52571, Saudi Arabia
[c] Department of Biochemistry, Computational Medicinal Chemistry Laboratory, UCSS, Abdul Wali Khan University, Mardan, Pakistan
[d] Faculty of Pharmacy, AIMST University, Kedah, 08100, Malaysia
[e] Dr. Panjwani Center for Molecular Medicine and Drug Research, International Center for Chemical and Biological Sciences, University of Karachi, Karachi, 75270, Pakistan
[f] Department of Clinical Pharmacy, Institute for Research and Medical Consultations (IRMC), Imam Abdulrahman Bin Faisal University, P.O. Box 1982, Dammam, 31441, Saudi Arabia

ARTICLE INFO

Article history:
Received 14 June 2019
Received in revised form
9 August 2019
Accepted 2 September 2019
Available online 5 September 2019

Keywords:
Benzotriazoles
α-Amylase inhibition
α-glucosidase inhibition
Diabetes
In silico studies
Kinetic studies

ABSTRACT

Benzotriazoles (**4**–**6**) were synthesized which were further reacted with different substituted benzoic acids and phenacyl bromides to synthesize benzotriazole derivatives (**7**–**40**). The synthetic compounds (**7**–**40**) were characterized *via* different spectroscopic techniques including EI-MS, HREI-MS, ^{1}H-, and ^{13}C NMR. These molecules were examined for their anti-hyperglycemic potential hence were evaluated for α-glucosidase and α-amylase inhibitory activities. All benzotriazoles displayed moderate to good inhibitory activity in the range of IC_{50} values of 2.00–5.6 and 2.04–5.72 μM against α-glucosidase and α-amylase enzymes, respectively. The synthetic compounds were divided into two categories **"A"** and **"B"**, in order to understand the structure-activity relationship. Compounds **25** ($IC_{50} = 2.41 \pm 1.31$ μM), ($IC_{50} = 2.5 \pm 1.21$ μM), **36** ($IC_{50} = 2.12 \pm 1.35$ μM), ($IC_{50} = 2.21 \pm 1.08$ μM), and **37** ($IC_{50} = 2.00 \pm 1.22$ μM), ($IC_{50} = 2.04 \pm 1.4$ μM) with chloro substitution/s at aryl ring were found to be most active against α-glucosidase and α-amylase enzymes. Molecular docking studies on all compounds were performed which revealed that chloro substitutions are playing a pivotal role in the binding interactions. The enzyme inhibition mode was also studied and the kinetic studies revealed that the synthetic molecules have shown competitive mode of inhibition against α-amylase and non-competitive mode of inhibition against α-glucosidase enzyme.

1. Introduction

Diabetes mellitus (DM), is a most common and epidemic disorder of the century which effects the metabolic functions of the endocrine system. It is widely spread in all parts of the world and is increasing rapidly. Due to the damage of specialized cells (islets of langerhans) which are responsible to produce insulin in the human body, the diabetic patients either do not produce or are unable to utilize it properly. This dysfunction leads to high blood glucose (sugar) levels in the body leading to hyperglycemia. Diabetes may be of two types, insulin dependent which is due to lack of insulin production in the human body is called as type 1, however, in the type 2 diabetes the body system is either unable to produce or not utilizing the insulin properly. It is among the most common chronic diseases after cancer and cardiovascular diseases which leads to mortality [1,2].

Due high prevalence of diabetic, various approaches have been

* Corresponding author. H. E. J. Research Institute of Chemistry, International Center for Chemical and Biological Sciences, University of Karachi, Karachi, 75270, Pakistan.
E-mail addresses: khalid.khan@iccs.edu, drkhalidhej@gmail.com (K.M. Khan).

https://doi.org/10.1016/j.ejmech.2019.111677
0223-5234/

made to control and manage the disorders caused by it. However, inhibition of carbolytic enzymes such as α-glucosidase and α-amylase is one of the common approach to manage or minimize these metabolic disorders [3]. Amylase, protease, and lipase are most commonly used enzymes in industry, and food biotechnology [4,5]. α-Amylase (EC 3.2.1.1) an enzyme which catalyzes hydrolysis of polysaccharides, commonly starch to glucose and maltose [6]. It belongs to the family of metalloenzyme having calcium atom as a metal co-factor [5]. Starch is absorbed into our body by the hydrolytic action of α-amylase followed by the action of intestinal α-glucosidase enzyme [4]. Inhibitors of α-amylase function by modulating the blood glucose level after a meal. Thus potential inhibitors of α-amylase enzyme can be used clinically as chemotherapeutic agents for the treatment of diabetes as well as obesity [6,7].

Besides the use of multiple approaches, α-glucosidase (EC 3.2.1.20) enzyme inhibitors are amongst the alternative therapeutic method [8] used clinically for the treatment of diabetes. The inhibitors of this enzyme slow down the digestion process thus resulting in the slow absorption of glucose. Acarbose and miglitol are among the most common α-glucosidase inhibitors used clinically to reduce postprandial blood glucose level (Fig. 1). These clinical drugs inhibit formation of glucose in the small intestine by inhibiting α-glucosidase enzyme. Acarbose, an anti-diabetic drug and tetrasaccharide mimic, with potent α-amylase and α-glucosidase inhibitory activity is used currently in the treatment of T2DM [9]. However, various side effects including flatulence and abdominal pain are related with acarbose. These side effects often limit the use of drug alone, thus used in combination with other anti-diabetic medicines to improve the efficacy. Thus, there is a dire need to design and develop a more potential molecules having less side effects to cure diabetes mellitus [10].

The heterocyclic scaffold as being the center for pharmacological activity have attracted a considerable attention of medicinal chemist. Triazoles are heterocyclic compounds composed of a five-membered unsaturated ring with three nitrogen and two carbon atoms at non-adjacent positions. Triazoles exist in different isomeric forms based on the position of nitrogen (N) atoms in the ring [11,12]. Since decades, triazoles and its related compounds have attracted great attention of chemists as well as biologists due to their chemotherapeutical importance [13,14]. The literature search reveals that 1*H*-1,2,3-triazoles nucleus is a core structural component in number of drugs having different pharmacological properties such as antiinflammatory, antimicrobial, antiviral, and antiparasitic. These molecules also found to have analgesic effects along with antineoplastic, anaesthetic, antiepileptic, antidepressant, antioxidant, anti-Parkinson's, anti-diabetic, and anti-obesity properties (Fig. 2) [15–17].

Heterocyclic compounds are of special interest to medicinal chemists due to their exceptional chemical and versatile biological profiles. Therefore, our research group had explored large number of heterocyclic organic molecules of different category and classes in search of their potential uses in medicinal chemistry [17–24]. In the recent past, we had identified and reported benzimidazoles, pyrazolones, and imidazoles as potential α-glucosidase and α-amylase inhibitors (Fig. 3) [18]. Keeping in mind the α-glucosidase potential of benzimidazoles and related compounds, we deliberately designed, synthesized, and evaluated 1,2,3-triazoles (benzotriazole) for α-amylase and α-glucosidase inhibition in order to identify lead molecules which may act as dual inhibitors. The treatment of diabetic patients often need (medicine) a combination therapy due to the slow healing process. Therefore, it is still need to explore more compounds for this disease in order to develop lead candidates to carry out some advance research in future. Thus, we decided to screen a library of substituted 1,2,3-benzotriazoles (**7**–**40**) and found that many compounds are dual inhibitors of α-glucosidase and α-amylase enzymes.

2. Results and discussion

2.1. Chemistry

Benzotriazoles **7**–**40** were synthesized by treating benzene-1,2-diamines (**1**–**3**) with CH_3COOH and $NaNO_2$ to give different substituted benzotriazoles (**4**–**6**). Benzotriazoles were then reacted with different substituted phenacyl bromides in ethanol and triethylamine at 60–70 °C to give *N*-substituted benzotriazoles derivatives (**25**–**40**). Benzotriazoles (**4**–**6**) were also treated with different substituted benzoic acid in the presence of CDI (1,1′-carbonyldiimidazole) as coupling agent in acetonitrile at 70–80 °C. The carboxylic group of acid was converted into good leaving group by treating it with coupling reagent CDI. In this reaction, acid imidazole reactive intermediate was formed, and carbon dioxide (CO_2) is liberated afterward the elimination of imidazole ring takes place. The acid imidazole being unstable reacts immediately with 1,2,3-triazoles to afford *N*-substitued benzotriazoles (**7**–**24**) (Scheme 1). All synthetic benzotriazoles (**7**–**40**) were fully characterized by different spectroscopic techniques including ^1H, ^{13}C NMR, EI-MS, HREI-MS, and IR.

2.2. EI-MS spectrometry of characteristic compound

EI-MS spectra of compounds **8** and **28** of category **A** and **B**, respectively, were discussed below. EI-MS spectra of compound **8** showed the molecular ion peak at *m/z* 325 for molecular formula $C_{13}H_6Cl_3N_3O$. The two isotopic peaks [M^++2] and [M^++4] due to the presence of chlorine atoms were appeared at *m/z* 327 and 329, respectively. The significant fragment appeared at *m/z* 289 by the loss of chlorine. Another fragment appeared at *m/z* 185 confirms the formation of 3,4-dichloro-1*H*-benzo[d] [1–3] triazole, while, the formation of 1-(3-chlorophenyl) ethan-1-one was confirmed by the significant fragment at *m/z* 139 (Fig. 4).

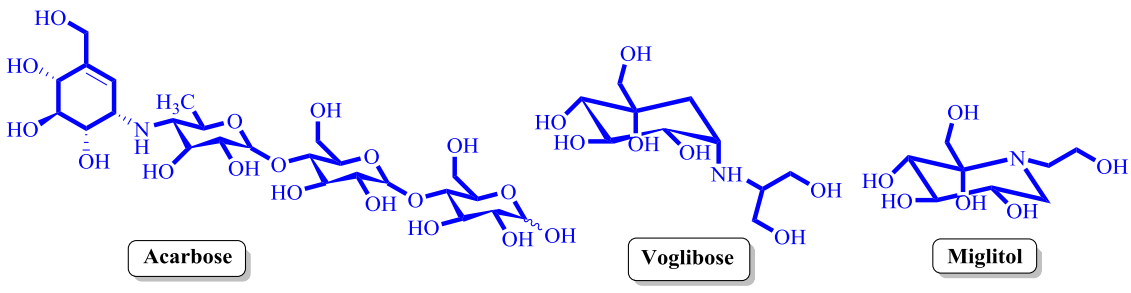

Fig. 1. Clinical medicine for the therapeutic of type II diabetes mellitus.

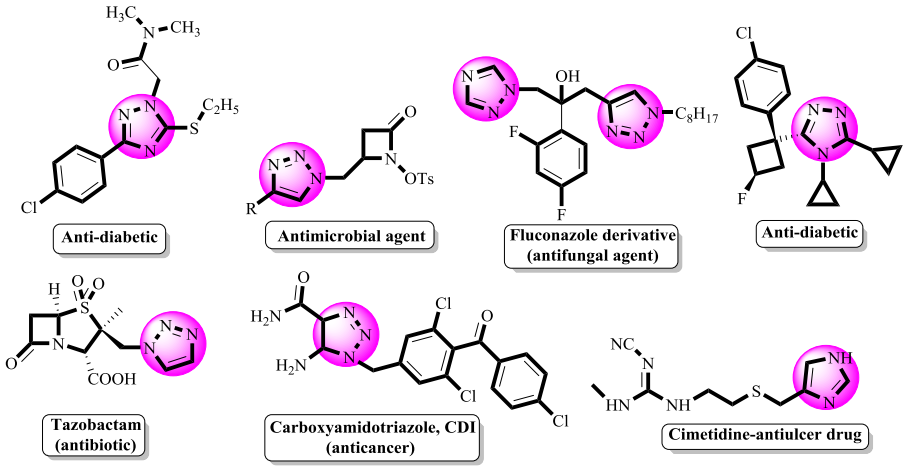

Fig. 2. 1,2,3-triazole containing commercial drugs and bioactive molecules.

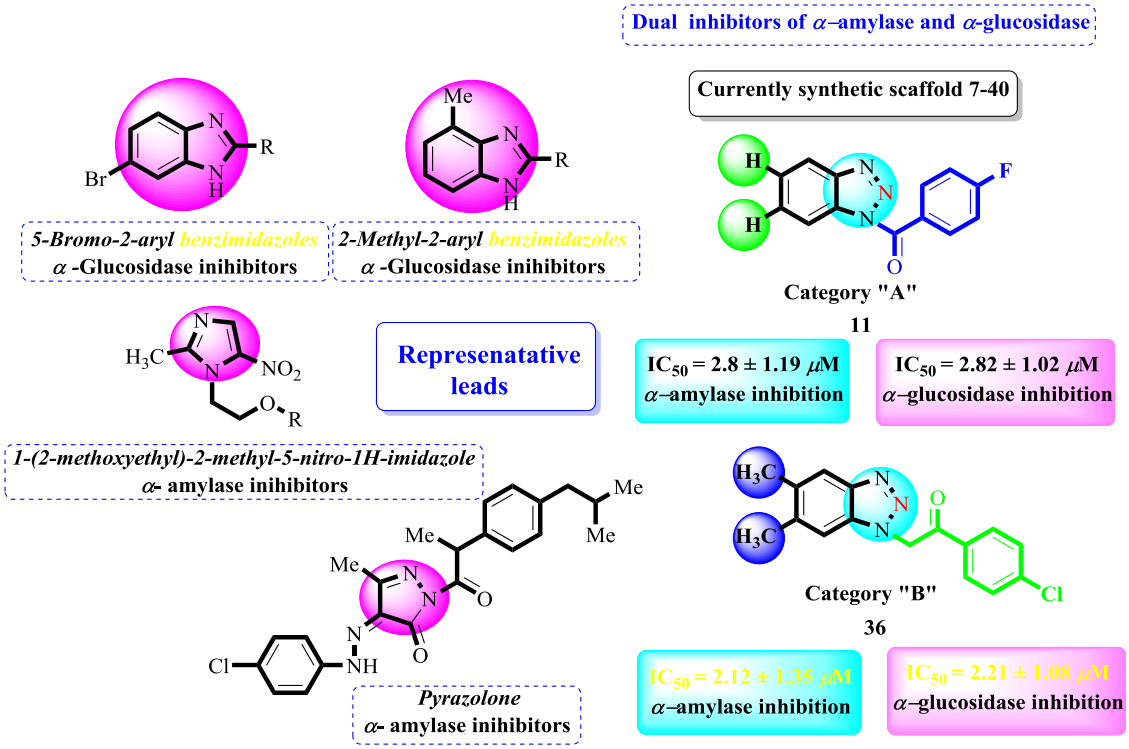

Fig. 3. Rationale of the current Study.

EI-MS spectra of compound **28** from **"Category B"**, showed the molecular ion peak at *m/z* 315 for molecular formula $C_{14}H_{10}BrN_3O$. The $[M^+ + 2]$ isotopic peak of bromine was appeared at *m/z* 317. The significant fragment appears at *m/z* 236 by the loss of bromine atom. The fragment appeared at *m/z* 133 confirms the formation of 1-methyl-1*H*-benzo[d] [1–3] triazole, while the formation of 3-bromobenzaldehyde was confirmed by the significant fragment at *m/z* 183. The key fragments are presented in (Fig. 4).

2.3. ^1H NMR

2.3.1. "Category A"

The ^1H NMR spectrum of compound **8** was recorded in (DMSO-d_6) on a Bruker AM 300 MHz instrument (Fig. 5). The most downfield singlets of two CH protons of benzotriazole ring resonated at δ_H 8.79 and 8.51, respectively. The molecule comprises of an aryl ring having 4 protons, among them, signal of proton H-6′ appeared at δ_H 8.12 as triplet ($J_{6',2'/6',4'} = 1.8$ Hz, 1H, H-6′), showing *meta*, coupling with H-2′ & H-4′. While, C-2′ and C-4′ protons were resonated at δ_H 7.87 ($J_{4',3'} = 7.2$ Hz, $J_{4',6'} = 1.2$ Hz) and 8.06 ($J_{2',3'} = 7.8$ Hz) as double doublet and doublet, respectively. However, H-3′ appeared at δ 7.71 as triplet showing coupling with H-2′ and H-4′ having coupling constant $J_{3',2'/3',4'} = 8.1$ Hz (Fig. 5).

^1H NMR spectrum of compound **28** was recorded in DMSO-d_6 on a Bruker AM 300 MHz instrument (Fig. 6). The compound comprises of the total ten protons, the most downfield proton H-2′

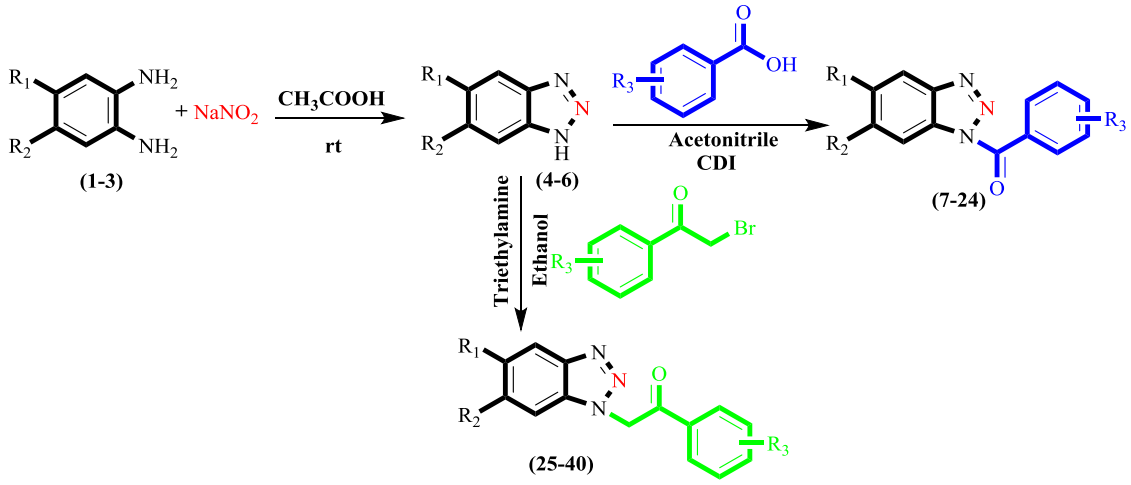

Scheme 1. Synthesis of novel benzo-1,2,3-triazoles derivatives (**7**–**40**).

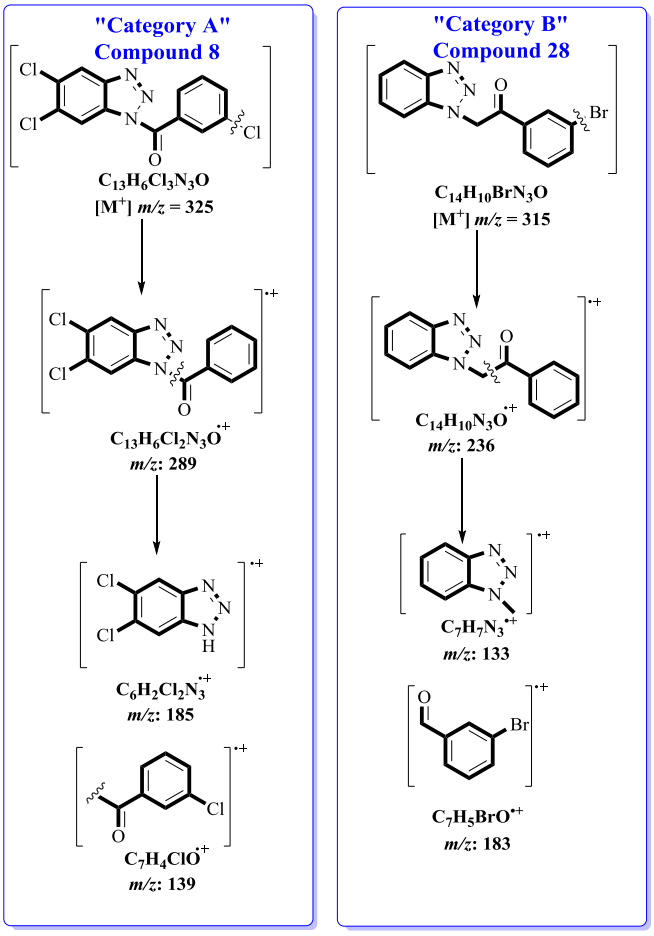

Fig. 4. Key fragmentation of representative compounds **8** and **28**.

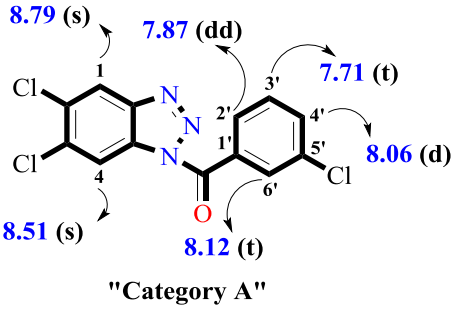

Fig. 5. ^{1}H NMR chemical shifts of representative compound **8**.

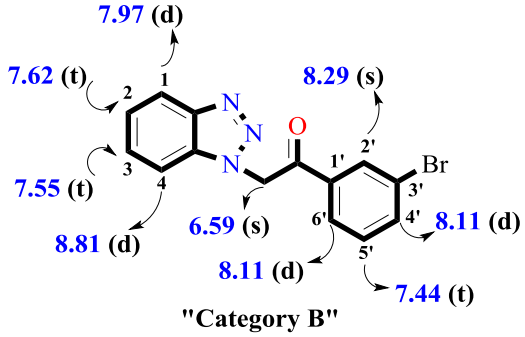

Fig. 6. ^{1}H NMR chemical shifts of representative compound **28**.

showing a singlet and appeared at δ 8.29. The other two aromatic proton H-4′ and H-6′ of acteophenone ring also resonated at δ_H 8.11 ($J_{6',5'/4',5'} = 7.5$ Hz) as a doublet showing *ortho*, coupling with H-5′, respectively. H-1 and H-4 protons of benzotriazole ring were the most downfield due to presence of three nitrogen atoms in the triazole ring and resonated as δ_H 7.97 and δ_H 7.81 as doublet, respectively. The H-2 resonated at δ_H 7.62 as triplet with coupling constant value of 7.8 Hz showing coupling with H-1 and H-3, respectively, however, H-3 resonated at δ_H 7.55 ($J_{2(1,3)} = 7.8$ Hz). However, H-5′ of acetophenone moiety appeared at δ 7.44 as triplet showing coupling with H-4′ and H-6′ with coupling constant value of 7.8 Hz. The CH_2 protons were resonated as a singlet at δ_H 6.59 (Fig. 6).

2.4. *In vitro* α-amylase and α-glucosidase inhibitory activities

All synthetic benzotriazoles derivatives (**7**–**40**) were screened for *in vitro* α-amylase and α-glucosidase inhibitory activities. It is noteworthy that all benzotriazole compounds displayed moderate to good inhibitory activity against both enzymes as compared to standard acarbose (Table-1). The synthetic derivatives have been

divided into two categories in order to understand the better structure-activity relationship (SAR). **"Category A"** comprises of eighteen derivatives (**7**–**24**) that are derived from reaction of benzotriazole with different substituted benzoic acids having an amide bond, while **"Category B"** is composed of sixteen molecules (**25**–**40**) synthesized *via* reaction of benzotriazole with phenacyl bromides possessing active methylene and acetophenone part (Fig. 7). The limited structure-activity relationship (SAR) suggested that all structural features such as benzotriazole ring, amide group, acetophenone, and aryl part are actively participating in the activity and any variation in the activity is attributed to the different substitution groups on aryl ring (R_3) and benzotriazole part (R_1 and R_2).

2.5. Structure-activity relationship (SAR) for α-amylase inhibitory activity

For each category, limited structure-activity relationship was discussed based on variable substituted "R" groups. Since, the results revealed that the main and persistent structural features in both categories such as (benzotriazole ring, amide, and acetophenone moiety) are taking important role in the (SAR) for α-amylase inhibitory activity, nonetheless, the variation in the activities is the result of variable features at benzotriazole (**R_1, R_2**) and aryl rings (**R_3**).

2.5.1. "Category A"

Compounds **8**, **9**, and **10** having chloro substituted benzotriazole ring exhibited potential inhibitory activity. Among them, compound **8** ($IC_{50} = 2.99 \pm 1.43\ \mu M$) with chloro substitution at *meta* position of aryl part was found to be most active. However, compounds **9** ($IC_{50} = 3.66 \pm 1.18\ \mu M$) and **10** ($IC_{50} = 3.66 \pm 1.04\ \mu M$) bearing unsubstituted and dimethyl substituted phenyl ring showed comparable activity with respect to each other but decreased activity as compared to compound **8**. The enhanced activity of compound **8** might be due to three chloro groups which help in better interaction of molecule within the enzyme's pocket, removal of chloro group or replacing chloro group with methyl resulted in decreased activity as in compounds **9** and **10**.

Compound **7** ($IC_{50} = 3.32 \pm 1.32\ \mu M$) having dimethyl substituted benzotriazole ring and unsubstituted aromatic ring displayed comparable activity with the standard acarbose ($IC_{50} = 2.00 \pm 1.35\ \mu M$). However, it was less active as compared to compound **9**, might be the replacement of chloro groups with methyl at benzotriazole ring were responsible for the slight decreased activity (Fig. 8).

Compounds **11**, **12**, **13**, and **14** with unsubstituted benzotriazole ring and different halogen substituents at different position of aryl ring were found to have varying degree of inhibitory potential. Amongst them, *para* fluoro substituted compound **11** ($IC_{50} = 2.8 \pm 1.19\ \mu M$) showed potential inhibition as compared to the standard acarbose ($IC_{50} = 2.00 \pm 1.35\ \mu M$). Compound **11** was also found to be most active compound of the **"Category A"**, might be unsubstituted benzotriazole part and substitution of fluoro group have attained a favorable confirmation susceptible for making π-π and other interactions with enzyme's active site (Fig. 9). However, difluoro substituted compound **13** ($IC_{50} = 5.00 \pm 1.18\ \mu M$) bearing both fluoro groups at *ortho* positions of aryl ring showed almost two folds less activity as compared to compound **11**. The decreased activity might be due to change in position of fluoro group and addition of another group resulted in increased steric factor resulting it less suitable to interact with active site of enzyme. Compound **12** ($IC_{50} = 5.72 \pm 1.12\ \mu M$) with additional chloro and fluoro at *ortho* and *meta* positions, respectively, displayed further declined activity as compared to compound **11** and **13** which again showed that increasing the number of substituents leads to decreased activity. Compound **14** ($IC_{50} = 3.13 \pm 1.18\ \mu M$) with bromo group at *para* position was slightly less active as compared to fluoro substituted compound **11**.

Compounds **15** and **16** having methoxy substitutions showed variable degree of inhibition. Amongst them compound **15** ($IC_{50} = 2.98 \pm 1.09\ \mu M$) bearing methoxy group at *para* position was the second most active compound of this category which indicates that *para* methoxy moiety may interacted more proficiently with the enzyme. The change in position of methoxy from *para* to *ortho* in compound **16** ($IC_{50} = 4.77 \pm 1.30\ \mu M$), however, displayed decreased activity. Replacement of methoxy with methyl group at different position of aryl part also resulted in decreased activity. Compounds **17** ($IC_{50} = 4.3 \pm 1.15\ \mu M$) with *meta*-methyl group displayed less activity as compared to the standard acarbose. The addition of another methyl group at *para* position as in compound **18** ($IC_{50} = 4.73 \pm 1.22\ \mu M$) resulted in further decrease in activity. Interestingly, compound **19** ($IC_{50} = 4.12 \pm 1.23\ \mu M$) with three methyl groups adjacent to each other was slightly more active as compared to compound **17** (Fig. 10).

Compound **20** ($IC_{50} = 2.92 \pm 1.81\ \mu M$) with *para* nitro substitution demonstrated better α-amylase inhibitory activity as compared to compound **21** ($IC_{50} = 4.08 \pm 1.09\ \mu M$) having an additional methyl group showed less activity which confirmed that methyl group are not contributing in the activity. Incorporation of amino and chloro groups as in compound **22** ($IC_{50} = 4.28 \pm 1.45\ \mu M$) also lead to slight decreased α-amylase inhibitory potential. However, compounds **23** ($IC_{50} = 5.4 \pm 1.40\ \mu M$) and **24** ($IC_{50} = 5.38 \pm 1.4\ \mu M$) with butoxy, and unsubstituted phenyl ring also found to be less active (Fig. 11).

2.5.2. "Category B"

Compounds **25**–**40** belong to **"Category B"**. In this category, compound **25** ($IC_{50} = 2.41 \pm 1.31\ \mu M$), with mono chloro substitutions at aryl part and unsubstituted benzotriazole ring, respectively, showed good inhibitory potential. However, addition of another chloro group to the adjacent position as in compound **26** ($IC_{50} = 3.89 \pm 1.09\ \mu M$) resulted in a decreased activity. Shifting the position of chloro group from *para* to *ortho* as in compound **27** ($IC_{50} = 3.51 \pm 1.12\ \mu M$) leads to slight better activity (Fig. 12). Compound **28** ($IC_{50} = 2.76 \pm 1.04\ \mu M$) bearing bromo group at *para* position displayed almost comparable activity with compound **25**. Its structurally similar analogue **29** ($IC_{50} = 4.35 \pm 1.09\ \mu M$) with *meta* bromo group at aryl ring showed almost two folds less activity which shows that substitution at *para* position might be helpful in better interaction with the active site of enzyme.

Compound **34** ($IC_{50} = 4.89 \pm 1.41\ \mu M$) having unsubstituted aryl part was found to exhibit good inhibitory activity. Compound **35** ($IC_{50} = 4.92 \pm 1.45\ \mu M$) with *para* phenyl substituted ring displayed almost similar activity to compound **34**. Compounds **30** ($IC_{50} = 4.9 \pm 1.5\ \mu M$) and **31** ($IC_{50} = 4.42 \pm 1.08\ \mu M$) with *ortho* hydroxy and *meta* nitro groups showed slightly variable activities. Among them compound **31** having nitro group was most active might be the electron withdrawing effect or the particular position of nitro group is contributing in the activity. However, in the methoxy and methyl substituted compounds **32** ($IC_{50} = 4.42 \pm 1.12\ \mu M$) and **33** ($IC_{50} = 4.56 \pm 1.51\ \mu M$) with substitution at *para* position compound **32** also exhibited good inhibitory activity as compared to compound **33** (Fig. 13).

Amongst methyl substituted benzotriazole derivatives, compounds **36** ($IC_{50} = 2.12 \pm 1.35\ \mu M$) with mono chloro substitutions was found to be most active derivative of **"Category B"**. Comparison of inhibitory activity of compound **36** with **25** ($IC_{50} = 2.41 \pm 1.31\ \mu M$) revealed that methyl groups at benzotriazole moiety in **36** played some important role in the inhibitory potential. These methyl groups might involve in some non-polar or

Table 1
In vitro α-amylase and α-glucosidase inhibitory activities of benzotriazoles (7–40).

Compounds	R_1	R_2	R_3	α-Amylase Inhibition $IC_{50} \pm SEM^a$ (μM)	α-Glucosidase Inhibition $IC_{50} \pm SEM^a$ (μM)
"Category A" 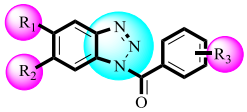					
7	**CH_3**	**CH_3**		3.32 ± 1.32	3.4 ± 1.09
8	**Cl**	**Cl**	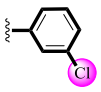	2.99 ± 1.43	3.00 ± 1.21
9	**Cl**	**Cl**	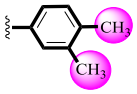	3.66 ± 1.18	3.82 ± 1.42
10	**Cl**	**Cl**		3.66 ± 1.04	3.7 ± 1.3
11	**H**	**H**	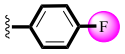	2.8 ± 1.19	2.82 ± 1.02
12	**H**	**H**	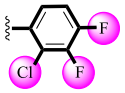	5.72 ± 1.12	5.63 ± 1.24
13	**H**	**H**	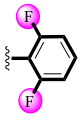	5.0 ± 1.18	5.23 ± 1.54
14	**H**	**H**	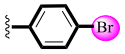	3.13 ± 1.01	3.2 ± 1.12
15	**H**	**H**	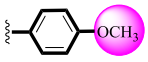	2.98 ± 1.09	2.99 ± 1.08
16	**H**	**H**		4.77 ± 1.3	4.79 ± 1.12
17	**H**	**H**	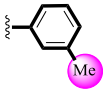	4.3 ± 1.15	4.42 ± 1.09
18	**H**	**H**	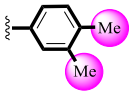	4.73 ± 1.22	4.8 ± 1.12
19	**H**	**H**	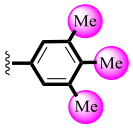	4.12 ± 1.23	4.23 ± 1.07
20	**H**	**H**	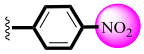	2.92 ± 1.81	2.97 ± 1.7
21	**H**	**H**	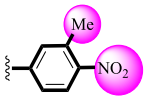	4.08 ± 1.09	4.1 ± 1.23
22	**H**	**H**	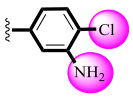	4.28 ± 1.45	4.32 ± 1.23

Table 1 (*continued*)

Compounds	R_1	R_2	R_3	α-Amylase Inhibition $IC_{50} \pm SEM^a$ (μM)	α-Glucosidase Inhibition $IC_{50} \pm SEM^a$ (μM)
23	**H**	**H**	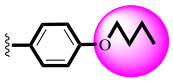	5.4 ± 1.40	5.6 ± 1.11
24	**H**	**H**		5.38 ± 1.4	5.29 ± 1.3
"Category B" 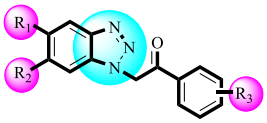					
25	**H**	**H**	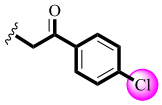	2.41 ± 1.31	2.5 ± 1.21
26	**H**	**H**	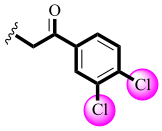	3.89 ± 1.09	3.9 ± 1.08
27	**H**	**H**	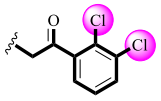	3.51 ± 1.12	3.47 ± 1.31
28	**H**	**H**	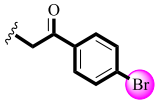	4.35 ± 1.09	4.41 ± 1.14
29	**H**	**H**	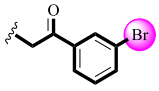	2.76 ± 1.04	2.79 ± 1.07
30	**H**	**H**	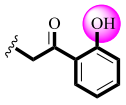	4.9 ± 1.5	4.87 ± 1.32
31	**H**	**H**	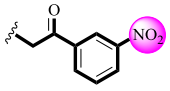	4.02 ± 1.08	4.00 ± 1.08
32	**H**	**H**	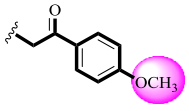	4.42 ± 1.12	4.5 ± 1.33
33	**H**	**H**	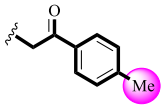	4.56 ± 1.51	4.78 ± 1.34
34	**H**	**H**	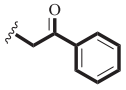	4.89 ± 1.41	4.91 ± 1.3
35	**H**	**H**	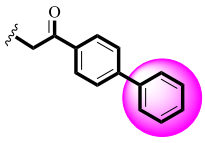	4.92 ± 1.45	4.98 ± 1.7

(*continued on next page*)

Table 1 (*continued*)

Compounds	R_1	R_2	R_3	α-Amylase Inhibition $IC_{50} \pm SEM^a$ (μM)	α-Glucosidase Inhibition $IC_{50} \pm SEM^a$ (μM)
36	**CH_3**	**CH_3**	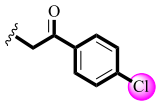	2.12 ± 1.35	2.21 ± 1.08
37	**CH_3**	**CH_3**	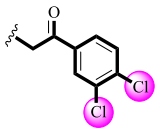	2.00 ± 1.22	2.04 ± 1.4
38	**CH_3**	**CH_3**	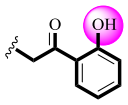	3.21 ± 1.32	3.3 ± 1.51
39	**CH_3**	**CH_3**	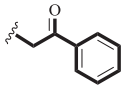	3.53 ± 1.31	3.41 ± 1.08
40	**CH_3**	**CH_3**	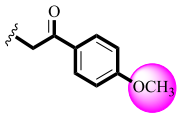	2.51 ± 1.82	2.6 ± 1.13
Standard = Acarbose				1.98 ± 1.04	2.00 ± 1.11

SEM[a] (Standard error of mean); (Standard inhibitor for α-amylase, α-glucosidase inhibitory activity).

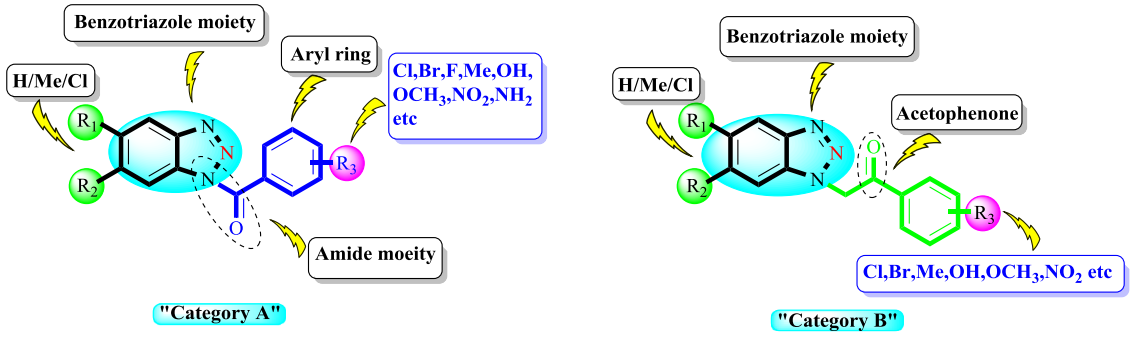

Fig. 7. General structure of synthetic benzotriazoles.

hydrophobic interactions with the active site of enzyme. Furthermore, compound **37** ($IC_{50} = 2.00 \pm 1.22$ μM) bearing an additional chlorine atom displayed increased activity as compared to compound **36**. Same activity pattern was observed when compared with compound **26** ($IC_{50} = 3.89 \pm 1.09$ μM) as it showed less inhibitory activity than derivative **36**. It further confirms the active participation of methyl group at benzotriazole ring.

Replacing chloro with methoxy as in compound **40** ($IC_{50} = 2.51 \pm 1.82$ μM) resulted in slight decreased activity (Fig. 7). Compounds **38** ($IC_{50} = 3.21 \pm 1.32$ μM) and **39** ($IC_{50} = 3.53 \pm 1.31$ μM) having *ortho* hydroxy group at aryl ring and unsubstituted aryl part were least active which indicate their weak interaction with active site of the enzyme (Fig. 14).

2.6. Structure-activity relationship (SAR) for α-glucosidase inhibitory activity

Compounds **7**–**24** of **"Category A″** demonstrated good α-glucosidase inhibitory activity in the range of $IC_{50} = 2.82 \pm 1.02$–5.63 ± 1.04 μM. All the structural features have actively participated in the activity of molecules (Fig. 15), however, slight variation in the activity is might be due to some variable structural features which played important role in the enzyme inhibition. A limited structure-activity relationship (SAR) was developed based on the variable groups and their particular positions on aryl ring. The synthetic compounds included in **"Category A″** have been composed of three different substituents on benzotriazole ring. Amongst chloro substituted benzotriazole derivatives of **"Category A″**, compound **10** ($IC_{50} = 3.7 \pm 1.3$ μM) with unsubstituted aryl ring exhibited good inhibitory activity. However, substitution on aryl part resulted in increased inhibitory activity as in compound **8** ($IC_{50} = 3.00 \pm 1.21$ μM) having chloro group at *meta* position might be due to better interaction of chloro group with active site of enzyme. Compound **9** ($IC_{50} = 3.82 \pm 1.42$ μM) with two methyl substituents *ortho* to each other was less active as compared to compound **8**, might be the methyl groups are creating steric hindrance or their electron donating effect is negatively participating in the activity. Compound **7** ($IC_{50} = 3.4 \pm 1.09$ μM) with unsubstituted aryl ring and methyl substituted benzotriazole ring displayed slight good inhibition as compared to compound **10** (Fig. 15).

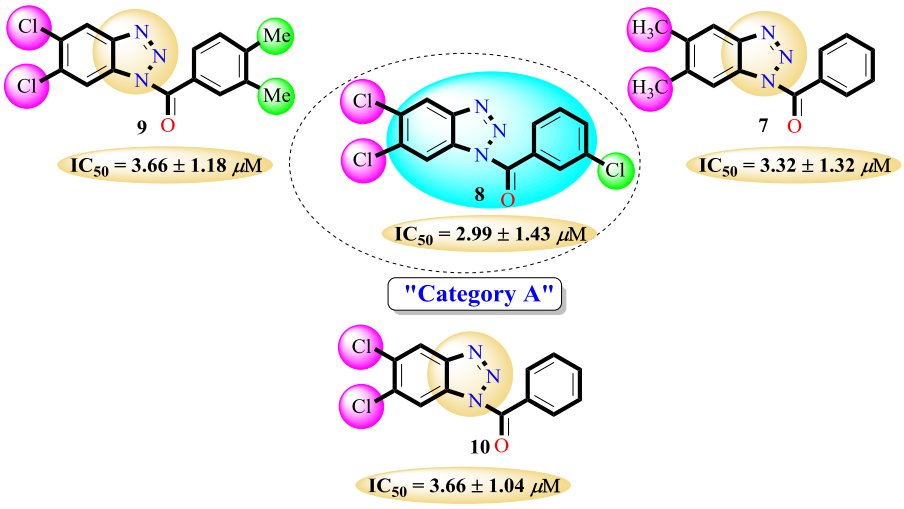

Fig. 8. Structure-activity relationship (SAR) of compounds 7-10.

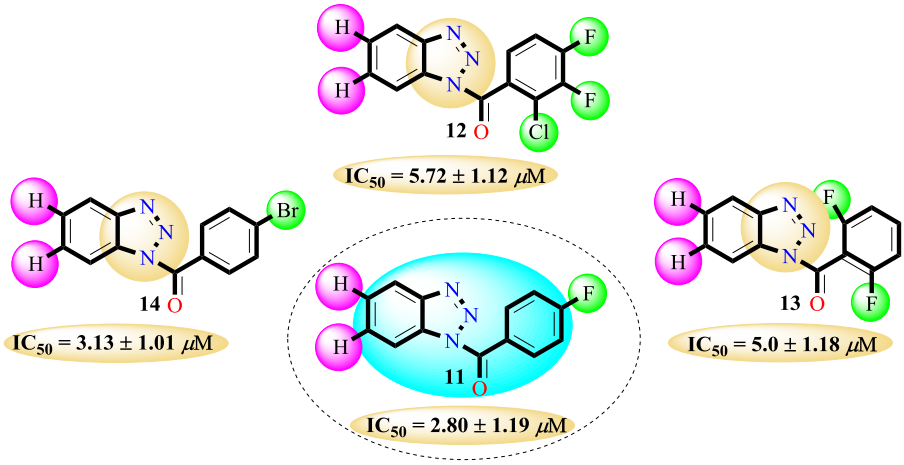

Fig. 9. Structure-activity relationship (SAR) of compounds 11-14.

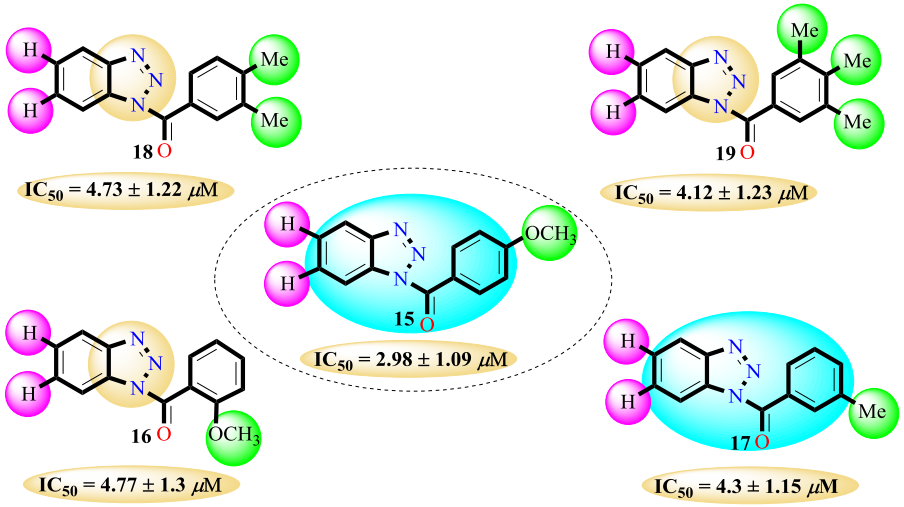

Fig. 10. Structure-activity relationship (SAR) of compounds 15-19.

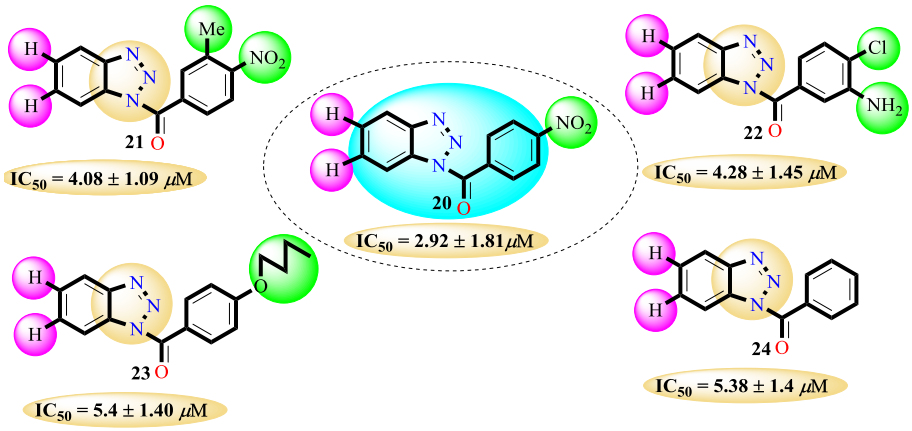

Fig. 11. Structure-activity relationship of compounds 20-24.

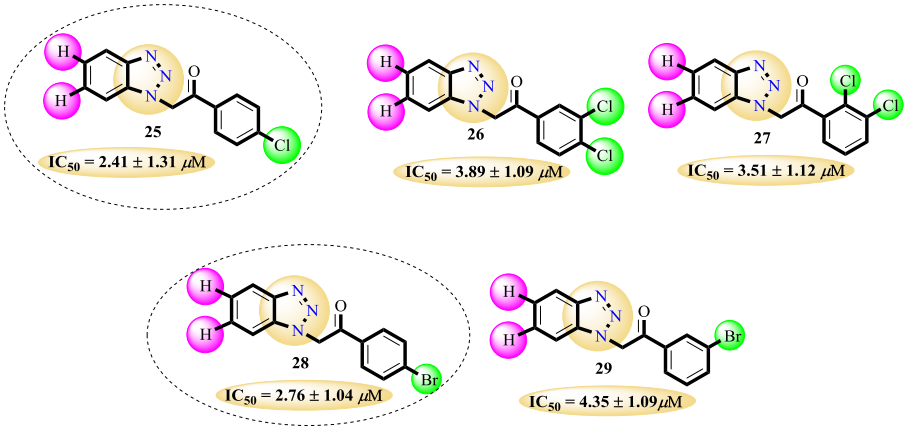

Fig. 12. Structure-activity relationship of compounds 25-29.

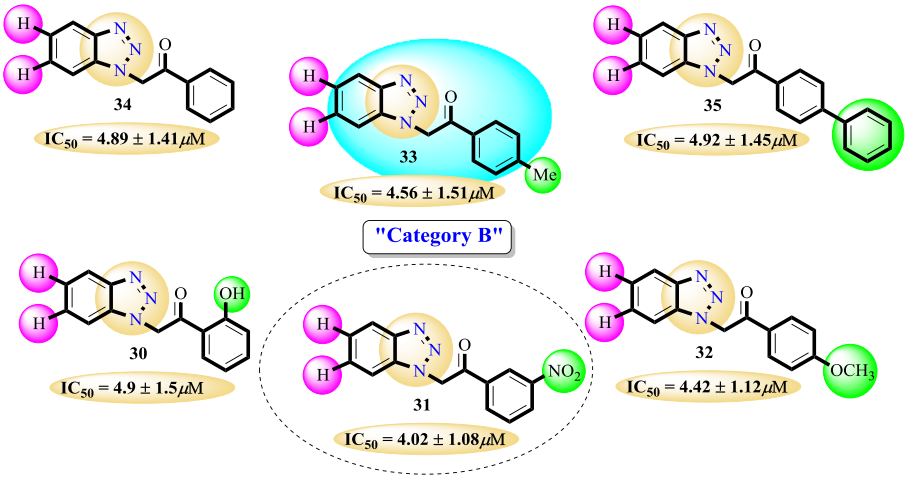

Fig. 13. Structure-activity relationship of compounds 30-35.

All other synthetic derivatives of this category are comprised of unsubstituted benzotriazole ring. Among them the *para* fluoro substituted compound **11** was found to be most active with IC_{50} value of $2.82 \pm 1.02\ \mu M$ and showed comparable activity to the standard acarbose ($IC_{50} = 2.20 \pm 1.11\ \mu M$). Changing the position and addition of flouro group resulted in two folds decreased activity in compound **13** ($IC_{50} = 5.23 \pm 1.54\ \mu M$) might be the *ortho* position is not favorable for the enzyme interaction. Adding chloro group along with two fluorine atoms in compound **12** ($IC_{50} = 6.63 \pm 1.24\ \mu M$) resulted in further declined activity which

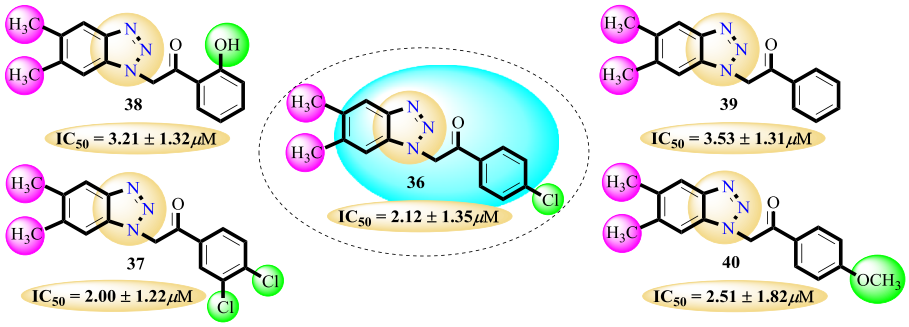

Fig. 14. Structure-activity relationship of compounds 36-40.

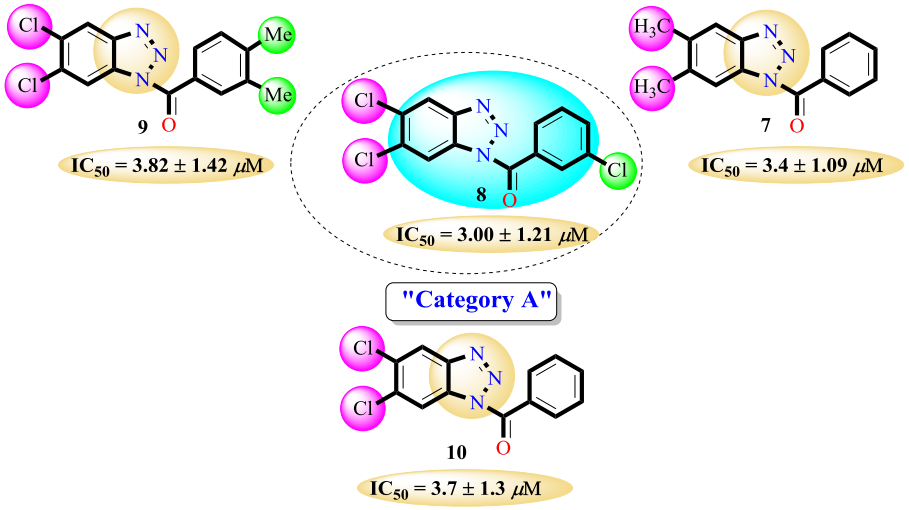

Fig. 15. Structure-activity relationship of compounds 7-10.

indicates that increasing number of substituents resulted in decreased activity might be due to increased steric factor. Replacing bromine with fluorine also resulted in decreased activity in compound **14** ($IC_{50} = 3.2 \pm 1.12\ \mu M$) (Fig. 16).

Compounds **15**–**19** with methoxy and methyl substituents also displayed variable inhibition against α-glucosidase. Compound **15** ($IC_{50} = 2.99 \pm 1.08\ \mu M$) with *para* methoxy group was more active as compared to its *ortho* methoxy derivative **16** ($IC_{50} = 4.79 \pm 1.12\ \mu M$) which showed that substituents at *para* position are actively participating in the activity and helping in the binding interactions of compounds with enzyme. However, methyl substituted analogs were moderately active as compared to methoxy substituted compounds. All three compounds **17** ($IC_{50} = 4.42 \pm 1.09\ \mu M$), **18** ($IC_{50} = 4.8 \pm 1.12\ \mu M$), and **19** ($IC_{50} = 4.23 \pm 1.07\ \mu M$) with mono, di, and trimethyl groups, respectively, displayed almost similar activity which showed that methyl groups are not actively participating in the activity (Fig. 17).

Compound **20** ($IC_{50} = 2.97 \pm 1.7\ \mu M$) with *para*-nitro substitution was second most active compound of **"Category A"**. The addition of methyl group adjacent to nitro as in compound **21** ($IC_{50} = 4.1 \pm 1.23\ \mu M$) resulted in decreased activity which again showed that methyl group are less participating in the activity. Compound **22** ($IC_{50} = 4.32 \pm 1.23\ \mu M$) having one chloro and amino group was placed *ortho* to each other was found to be less active against α-glucosidase enzyme. Compounds **23** ($IC_{50} = 5.6 \pm 1.11\ \mu M$) and **24** ($IC_{50} = 5.29 \pm 1.3\ \mu M$) with butoxy and unsubstituted phenyl ring were least active molecules of this category (Fig. 18).

Benzotriazoles derivatives **25**–**40** belongs to **"Category B"**. In this category, compound **25** ($IC_{50} = 2.5 \pm 1.21\ \mu M$) with *para* chloro substitution was most active which showed that substitution at *para* position is actively contributing in the activity. The di chloro compounds **26** ($IC_{50} = 3.9 \pm 1.08\ \mu M$) and **27** ($IC_{50} = 3.47 \pm 1.31\ \mu M$) with different positions of chlorine at aryl ring showed many folds decreased activity as compared to *para* chloro compound **25**. It showed that number and positions of the substituent played an important role in exhibiting the inhibitory potential. Interestingly, compound **28** ($IC_{50} = 2.79 \pm 1.07\ \mu M$) with *para* bromo substitution displayed almost similar activity as compound **25**. Changing the position of bromine atom from *para* to *meta* as in compound **29** ($IC_{50} = 4.41 \pm 1.14\ \mu M$) resulted in decreased activity. It was experienced that compounds with substituents having more negative inductive effect such as Cl, and Br showed more potent inhibition activity than the compounds with less negative inductive effect (Fig. 19).

Compound **34** ($IC_{50} = 4.91 \pm 1.3\ \mu M$) with unsubstituted phenyl ring was less active. However, compound **31** ($IC_{50} = 4.00 \pm 1.08\ \mu M$) bearing a *meta* nitro group exhibited good activity as compared to compound **34**. Replacing nitro group with *para* methoxy as in compound **32** ($IC_{50} = 4.5 \pm 1.33\ \mu M$) resulted in less activity might be due to the electron donating nature of the substituent. Compound **33** ($IC_{50} = 4.78 \pm 1.34\ \mu M$) with *para* methyl resulted in decreased activity as compared to methoxy substituted analog which showed that might be methoxy group is interacting with the

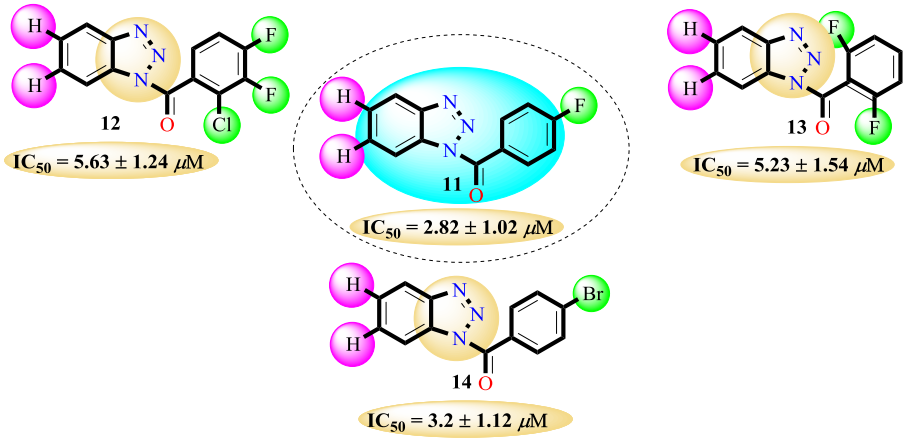

Fig. 16. Structure-activity relationship of compounds 11-14.

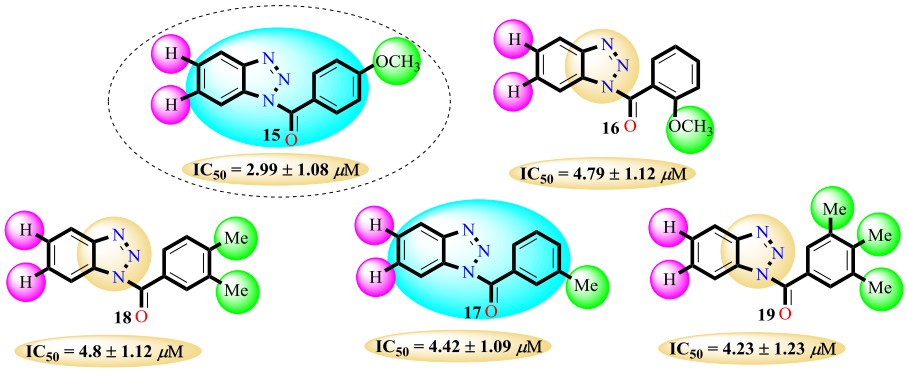

Fig. 17. Structure-activity relationship of compounds 15–19.

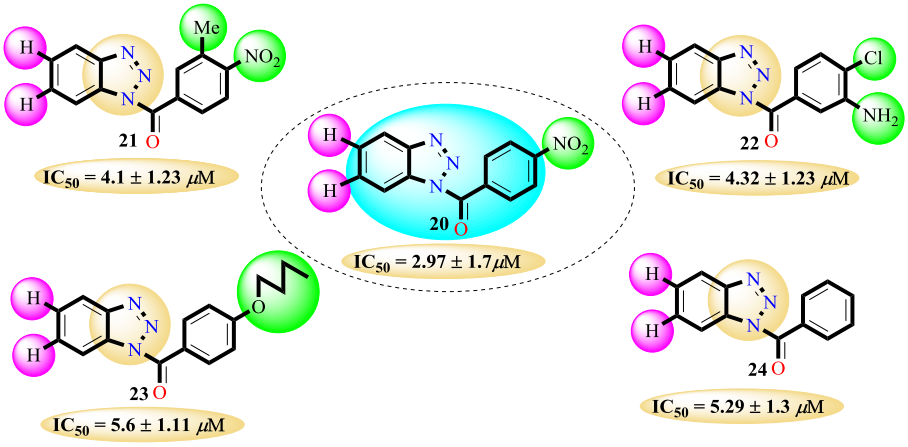

Fig. 18. Structure-activity relationship of compounds 20-24.

active site of enzyme through hydrogen bonding. Replacing methyl with phenyl ring resulted in further declined activity as in compound **35** ($IC_{50} = 4.98 \pm 1.7\ \mu M$). Compounds **30** ($IC_{50} = 4.87 \pm 1.32\ \mu M$) with *ortho* hydroxy group also displayed decreased activity (Fig. 20).

Compounds **36**–**40** were composed of methyl substituted benzotriazole ring, among them compound **36** ($IC_{50} = 2.21 \pm 1.08\ \mu M$) with *para* chloro substitution was found to be significantly active. As the results obtained in case of α-amylase inhibition, activity comparison of compound **36** with **25** ($IC_{50} = 2.5 \pm 1.21\ \mu M$) revealed that methyl substitutions are playing some role in the α-glucosidase inhibition. Similarly, compound **37** ($IC_{50} = 2.04 \pm 1.4\ \mu M$) with an additional chloro atom showed good α-glucosidase inhibition, however, it was better active as compared to compound **36**. Compound **38** ($IC_{50} = 3.3 \pm 1.51\ \mu M$) having *ortho* hydroxy group was found to be less active as compared to chloro

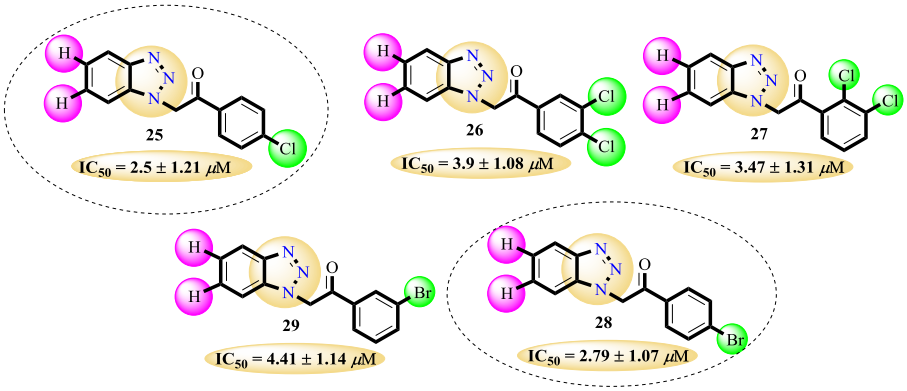

Fig. 19. Structure-activity relationship of compounds 25-29.

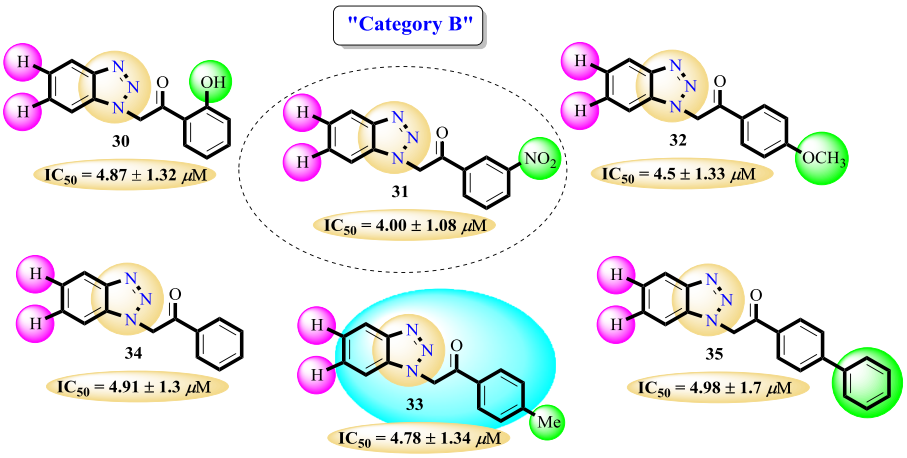

Fig. 20. Structure-activity relationship of compounds **30**–**35**.

substituted analogs. When *para* position was substituted with an electron-donating methoxy group in compound **40** ($IC_{50} = 2.6 \pm 1.13\ \mu M$) showed comparable activity to the standard acarbose, however, derivative **39** ($IC_{50} = 3.41 \pm 1.08\ \mu M$) with unsubstituted phenyl ring showed a weak inhibition activity as compared to other active compounds (Fig. 21) (see Fig. 22 and 23).

2.7. Kinetic characterization of α-amylase inhibition

Kinetic studies on the most active α-amylase inhibitors **40**, **37**, **36**, **25**, **29**, **11**, **20**, **15**, and **8** were analyzed to interpret the inhibition mechanism of these compounds The mechanism of enzyme inhibition was analyzed by graph fitting analysis using Sigma-Plot enzyme kinetic software. By using various kinetics plots such as Hanes-Woolf, Lineweaver-Burk, Hill, Scatchard, Eadie-Hofstee, and Dixon models, the kinetic parameters Km, AICc, Vmax, and R^2 values were calculated (Table-2). Based on curve fitting model and low AICc value, the kinetic studies results shown that all selected compounds following competitive type inhibitors mechanism (Fig. 24).

2.8. Kinetic characterization of α-glucosidase inhibition

Kinetic studies on the most active α-glucosidase inhibitors **40**, **31**, **30**, **19**, **23**, **7**, **14**, **9**, and **8** were analyzed to interpret the inhibition mechanism of these compounds. The mechanism of enzyme inhibition was analyzed by graph fitting analysis using Sigma-Plot enzyme kinetic software. By using various kinetics plots such as Lineweaver-Burk, Hill, Hanes-Woolf, Eadie- Hofstee, Dixon and Scatchard models, the kinetic parameters Vmax, Km, AICc and R^2 values were calculated (Table-3). Based on curve fitting model and low AICc value, the kinetic studies results shown that all selected compounds followed non-competitive type of inhibition mechanism (Fig. 25).

2.9. Molecular docking (MD) studies

2.9.1. α-Amylase molecular study

The MD approach was performed in-order to explore the possible binding mechanism of the competitive inhibitors against the α-amylase enzyme. The MD results revealed that all the inhibitors bind well to substrate binding site with various affinity. Based on visual inspection and PL interaction profile of all the inhibitors demonstrates that mostly, potent inhibitors possess electron withdrawing group in di or mono passion over benzene ring, the di-EWG groups (di-Cl) in compound **37** ($IC_{50} = 2.00 \pm 1.22\ \mu M$) showed best fit-well pattern of PL interaction profile and remain tight in the active site; the PL interaction profile includes residue Lys200, Ile235, His201, Tyr151, Asp300 as shown in Fig. 26A. The high potency of compound **37** might be due to the attached EWG di-Cl at *-para* and *-meta* position which readily draws electrons away from a reaction center, when this center is an electron rich carbanion, the presence of the electron-withdrawing substituent has a stabilizing effect, hence enhance the enzyme activity. In case

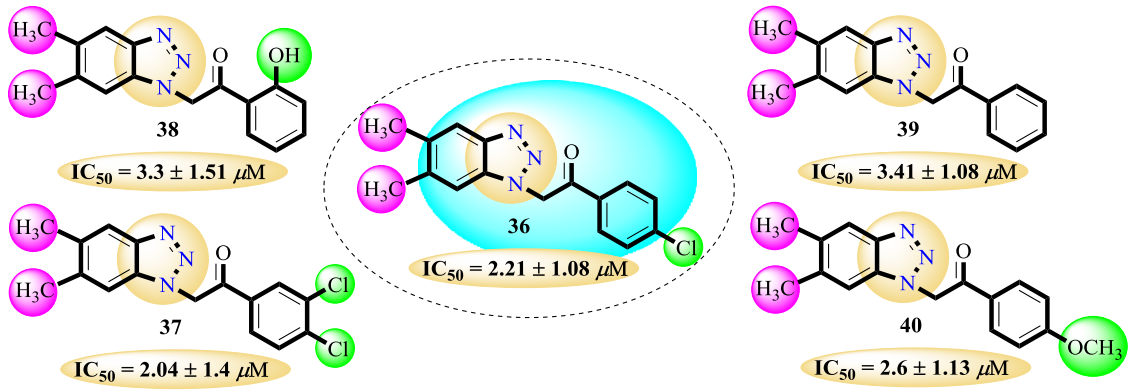

Fig. 21. Structure-activity relationship of compounds 36-40.

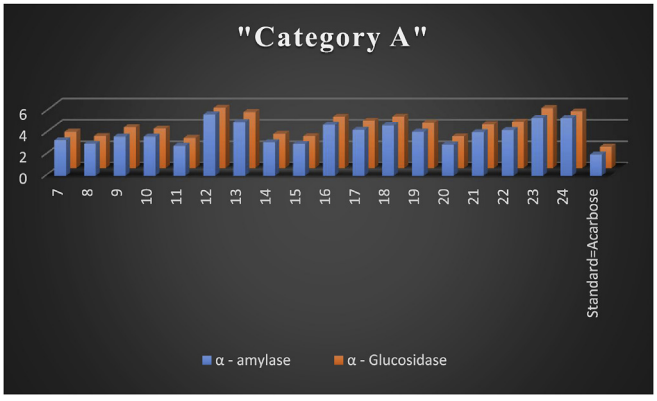

Fig. 22. Comparison of α-amylase and α-glucosidase activities of **"Category A"** compounds.

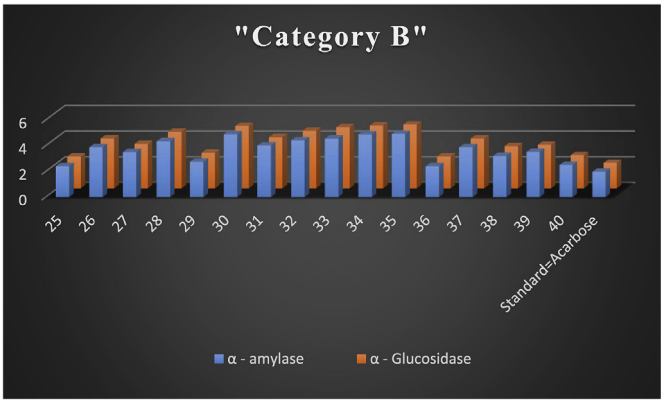

Fig. 23. Comparison of α-amylase and α-glucosidase activities of **"Category B"** compounds.

Table 2
Kinetic studies of active compounds for α-amylase inhibition.

S. No.	Compound No.	Vmax (μM/min)[1]	Km (mM)	AICc	R^2	Type of inhibition
1	**40**	505.1	0.20	202.4	0.912	Competitive type
2	**37**	593.3	0.24	214.2	0.924	Competitive type
3	**36**	514.4	0.18	210.1	0.920	Competitive type
4	**25**	527.0	0.20	202.8	0.910	Competitive type
5	**29**	512.5	0.21	208.2	0.914	Competitive type
6	**11**	522.2	0.19	210.8	0.902	Competitive type
7	**20**	511.6	0.20	230.2	0.914	Competitive type
8	**15**	554.0	0.21	220.4	0.908	Competitive type
9	**8**	514.5	0.20	230.5	0.914	Competitive type

of other top 3 out of 4 active inhibitors including **29**, **23**, **31** in the series adopt side chain donor and acceptor hydrogen interaction with residue Ile235, Glu233, Lys200, His201 (Fig. 26B-D). All these inhibitors possess the same EWG but the only differences found in position of attachment with mono-passion. As the position of the attached groups and their quantity (from mono to di or di to mono group) change ultimately reduce the catalytic activity. Overall, the MD study results demonstrate that the inhibitors possess higher number of attached groups over benzene showed not only high potency but as well as showed high potency experimentally. The detail protein-ligand interaction profile listed in Table-4.

2.9.2. α-Glucosidase molecular study

Molecular docking (**MD**) approach was performed to explore the possible binding mode of the synthetic derivatives against the α-glucosidase enzyme. Generally, the enlisted compounds possess different substituted groups, e.g., some possess electron withdrawing groups (**EWG**) and some have electron donating groups (**EDG**). The docking results revealed that the number of functional groups (mono to di or di to mono), position, and the variation in the substituted groups from one to another or *vice versa* eventually altered the enzyme activity. Subsequently, the MD results revealed that all the derivatives participated well in the binding with the catalytic residues that play a vital role in enhancing or reducing the activity of the enzyme. The MD resulted in further exploration of the binding pattern of all active compounds and were found well accommodated in the active site of the enzyme. The active compounds including compounds **37**, **36**, **25**, **40**, and **29** which ranked 1–5 in the series mainly showed significant interactions with the catalytic residues in the active sites of enzyme, respectively. The in-

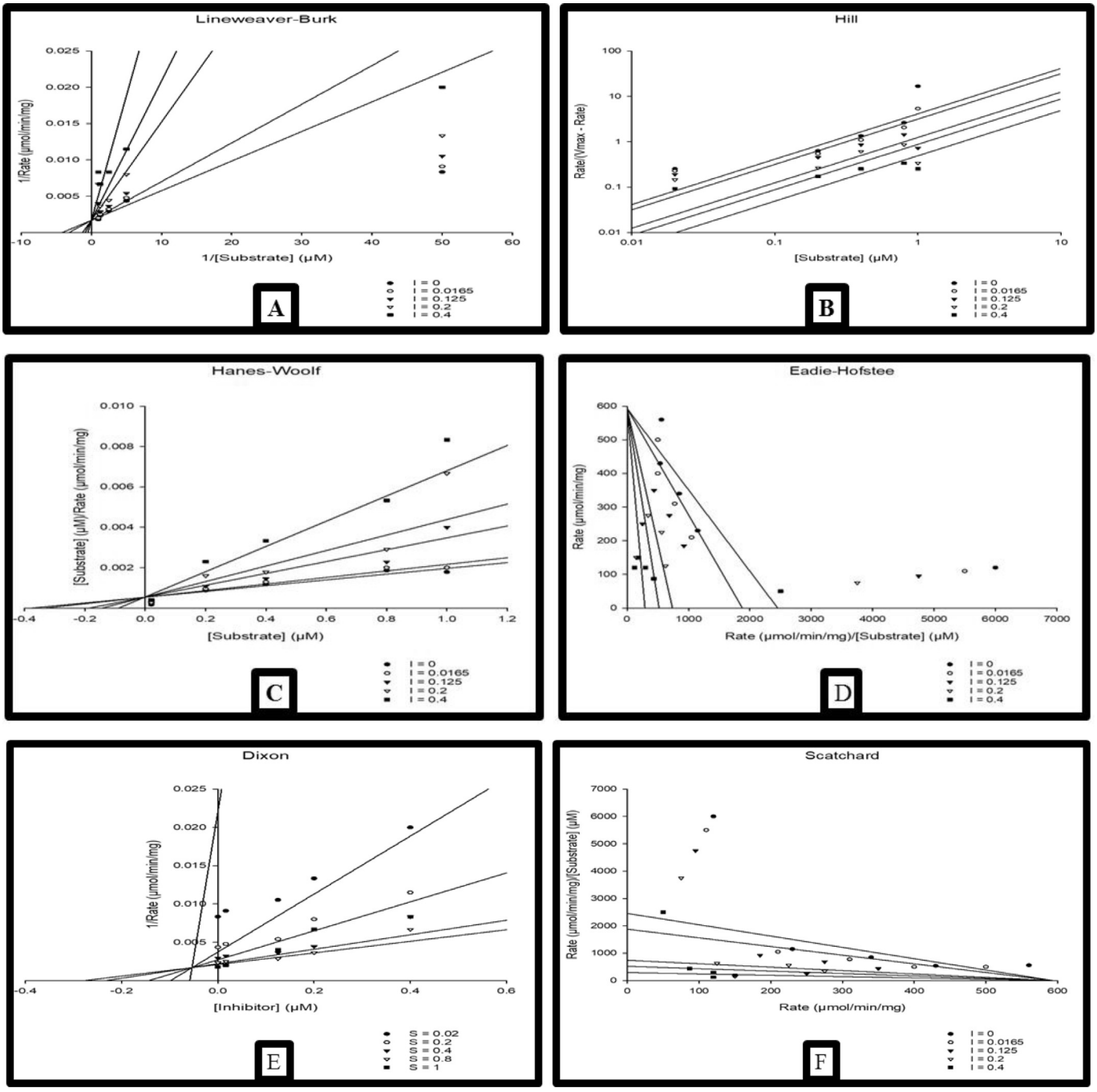

Fig. 24. A) Lineweaver-Burk plot of 1/[S] Vs 1/Rate in the different concentration of mixed-type inhibitor. **B**) Hill plot of different concentration of [S] Vs Rate (Vmax-Rate) in the different concentration of mixed-type inhibitor. Fig. 24: **C)** Hanes-Woolf plot of compound **8** at different concentration of [S] Vs [S]/Rate in the different concentration of mixed-type inhibitor. **D)** Eadie-Hofstee plot of compound **8** by rate/[S] Vs Rate in the different concentration of mixed-type inhibitor. Fig. 24: **E)** Dixon plot of compound **8** at different concentration of mixed inhibitor Vs 1/Rate. **F)** Scatard plot of compound **8** by Rate Vs Rate/[S] in the different concentration of mixed-type inhibitor.

depth protein-ligand interaction analysis for the most active compound **37** ($IC_{50} = 2.04 \pm 1.04\ \mu M$) demonstrates and support the high potency against α-glucosidase enzyme adopt most favorable interactions with active site catalytic residues, e.g., Glu276, Asp349, Asp408 and His245 (Fig. 27A). The high potency might be due to the attached EWG (di-Cl) and has more inductive effect as compare to compounds **36**, **25** and **29** which possess the same group at -*para* position but showed less activity (Fig. 27D). The low activity of these compounds as compared with the most potent compound **37** might be due to the quantity of the EWG and as well the position. In case of 2nd most active compound **25** which showed high activity than compound **29**, even though possess substituting group at -*para* position. The difference might be due to the inductive effect; the Cl have high than the Br.

Additionally, the compound Cl (3.16) have high electronegativity compared with Br (2.96). Based on the characteristics as mentioned earlier, the Cl tend to withdraw electron more efficiently than Br and hence enhance the enzyme activity. Moreover, similar protein-

Table 3
Kinetic studies of active compounds for α-glucosidase inhibition.

S. No.	Compound No	Vmax (μM/min)[1]	Km (mM)	AICc	R^2	Type of inhibition
1	**40**	620.1	0.21	210.1	0.902	Non-competitive type
2	**31**	618.4	0.26	203.3	0.914	Non-competitive type
3	**30**	601.2	0.25	212.0	0.925	Non-competitive type
4	**19**	612.5	0.20	221.3	0.940	Non-competitive type
5	**23**	620.8	0.24	205.4	0.912	Non-competitive type
6	**7**	602.2	0.20	211.5	0.951	Non-competitive type
7	**14**	612.5	0.20	214.2	0.926	Non-competitive type
8	**9**	620.2	0.24	218.1	0.902	Non-competitive type
9	**8**	620.3	0.25	205.4	0.940	Non-competitive type

ligand interaction profile was observed for other compounds, the only difference found in their activities might be due to residues interaction some interact with catalytic site residues and some with arbitrary residues in the active site which are less role in enhancing or reducing the enzyme activity, respectively.

Overall from the molecular docking approach, it was observed that all the derivatives showed enough favorable interactions. The observed gradual decreased in docking score as well as in the mode of interaction of each compound may be based on the attached electron withdrawing and donating groups, and hence participating in decreasing or enhancing the inhibition activity of the enzymes. The detail protein-ligands interaction profile listed in Table-5.

3. Conclusion

Thirty four benzotriazoles derivatives (**7**–**40**) were synthesized by reacting benzotriazoles with different substituted benzoic acids and phenacyl bromides. The synthetic compounds were evaluated for α-glucosidase and α-amylase inhibitory activities. All compounds displayed good to moderate inhibitory activities in the range of IC_{50} values of 2.00 ± 1.22–5.72 ± 1.12 and 2.04 ± 1.4–5.6 ± 1.11 μM against α-amylase and α-glucosidase enzymes, respectively. In order to understand better structure-activity relationship the synthetic compounds were divided into two categories **A** and **B**. Out of thirty four compounds, eight compounds **8**, **11**, **15**, **20**, **25**, **29**, **36**, and **40** displayed good inhibitory activities. These compounds displayed almost similar activity against α-amylase and α-glucosidase enzyme, thus found to have dual inhibitory activity. Molecular docking studies of most active compounds revealed that different substitutions at aryl ring are playing important roles in the binding interactions. The kinetic studies revealed that the synthetic molecules have shown competitive mode of inhibition against α-amylase and non-competitive mode of inhibition against α-glucosidase enzyme.

4. Experimental

4.1. Materials and methods

Thin layer chromatography was carried out on pre-coated silica gel, GF-254 (Merck, Germany). Spots were visualized under ultraviolet light at 254, 366 nm or iodine vapors. EI- and HREI-MS spectra were recorded on MAT 312 and MAT 113D mass spectrometers. The ^1H, ^{13}C NMR were recorded on a Bruker AM spectrometers, operating at 300 and 400 MHz. The chemical shift values are presented in ppm (δ), relative to tetramethylsilane (TMS) as an internal standard and the coupling constant (*J*) are in Hz. Melting points of the compounds were determined on a Stuart® SMP10 melting point apparatus and are uncorrected.

4.2. Kinetic study assay

4.2.1. α-Amylase inhibition assay

To determine the mechanism of enzyme inhibition, the kinetic studies were performed by using varying concentration of α-amylase inhibitors (0.0625, 0.125, 0.3 and 0.4 mM) with varying concentrations of inhibitor substrate (*p*-nitrophenyl-R-D-maltoside (NPM)) such as 0.1, 0.2, 0.4, 0.8, and 1.0 mM. The enzyme was dissolved in de-ionized water to produce the concentration 0.2 mg/mL for each well. PIPES buffer was to adjusted the pH at 7.0, the reaction mixture was incubated for the period of 30 min at 25 °C. The absorbance was measured using ELISA reader by keeping the 96-well plate (BioTek XL-800, USA). The kinetic parameters Vmax, Km, AICc and R^2 values of all the α-amylase inhibitor activities were determined by graph fitting analysis using Sigma-Plot enzyme kinetic software 14.0 version [24,25].

4.2.2. α-Glucosidase inhibition assay

To determine the mechanism of α-glucosidase enzyme inhibition, the kinetic studies were performed by using varying concentration of α-glucosidase inhibitors (0.0625, 0.125, 0.3 and 0.4 mM) with varying concentrations of inhibitor substrate (*p*-nitrophenyl R-D-maltoside (NPM)) such as 0.1, 0.2, 0.4, 0.8 and 1.0 mM. The enzyme was dissolved in de-ionized water to produce the concentration 0.2 mg/mL for each well. PIPES buffer was used as adjusted the pH of 7.0. the reaction mixture was incubated for the period of 30 min at 25 °C for 1-min interval. The absorbance was measured using ELISA reader by keeping the 96-well plate (BioTek XL-800, USA). The kinetic parameters Vmax, Km, AICc and R^2 values of all the α-glucosidase inhibitors were determined by graph fitting analysis using Sigma-Plot enzyme kinetic software 14.0 version [25].

4.2.3. α-Amylase inhibition assay

The α-amylase inhibitory activity was determined by an assay modified from Kwon, Apostolidis and Shetty. A volume of 500 μL of α-amylase solution (0.5 mg/mL) in 0.2 mM phosphate buffer (pH 6.9) and 500 μL of test sample (100, 200, 400, 800, 1000 μg/mL) were incubated for 10 min at 25 °C. After pre-incubation, 1% starch solution (500 μL) in 0.02 M sodium phosphate buffer (pH 6.9) was added to each tube and incubated at 25 °C for 10 min. 1 mL of dinitrosalicylic acid color reagent was then added to the reaction mixture and the tubes were incubated in boiling water for 5 min, and finally cooled to room temperature. The solutions were diluted by adding 10 mL distilled water and the absorbance was measured at 540 nm [9]. The percentage inhibition was calculated as illustrated,

$$\% \text{ Inhibition} = (\text{Absorbance}_{\text{Control}} - \text{Absorbance}_{\text{Sample}})/\text{Absorbance}_{\text{Control}} \times 100$$

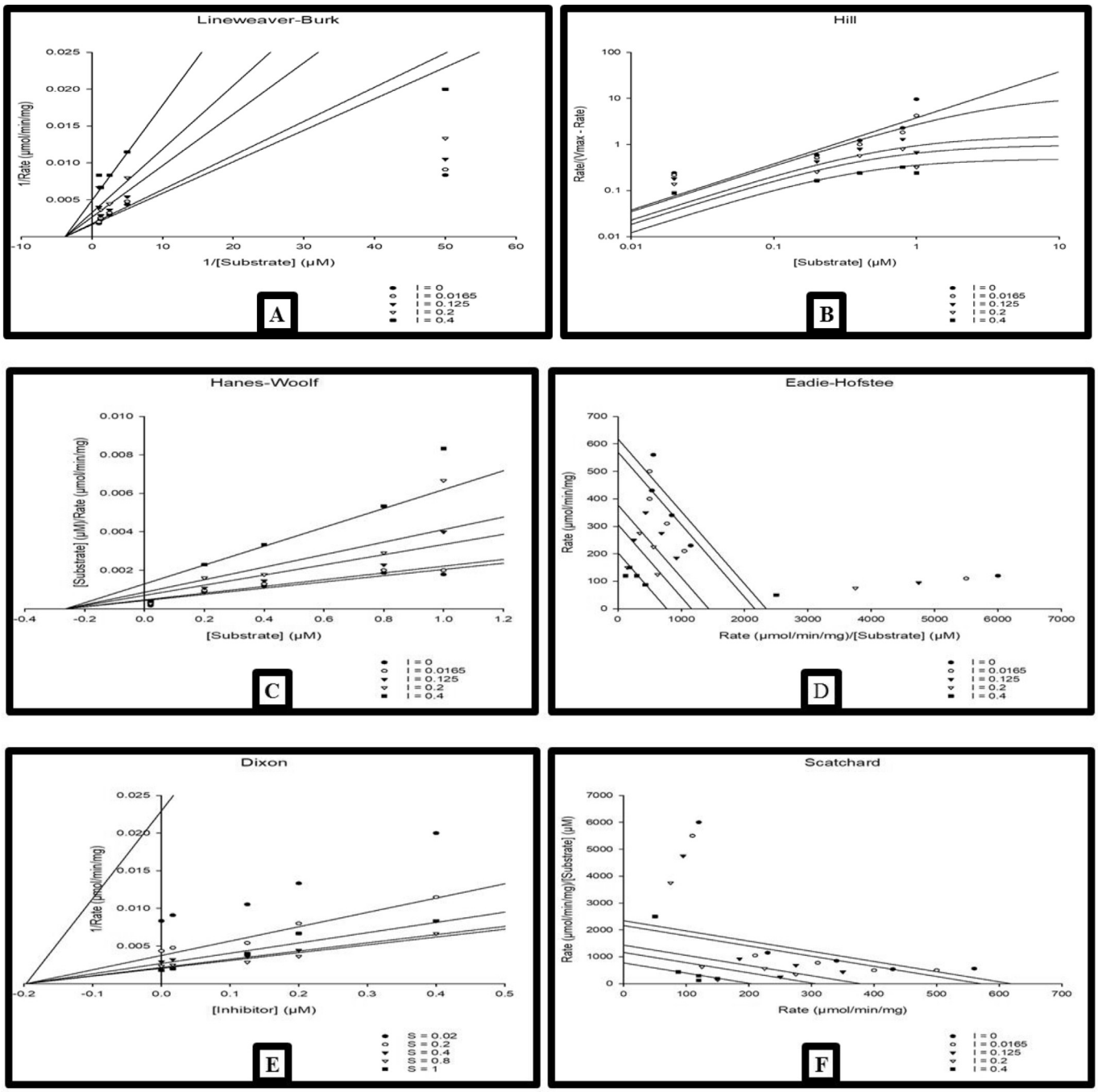

Fig. 25. A) Lineweaver-Burk plot of 1/[S] Vs 1/Rate in the different concentration of Competitive-type inhibitor. **B)** Hill plot of different concentration of [S] Vs Rate (Vmax-Rate) in the different concentration of Competitive-type inhibitor. Fig. 25 **C)** Hanes-Woolf plot of compound **8** at different concentration of [S] Vs [S]/Rate in the different concentration of competitive -type inhibitor. **D)** Eadie-Hofstee plot of compound **8** by rate/[S] Vs Rate in the different concentration of Competitive -type inhibitor. Fig. 25 **E)** Dixon plot of compound **8** at different concentration of Competitive Inhibitor Vs 1/Rate. **F)** Scatard plot of compound **8** by Rate Vs Rate/[S] in the different concentration of Competitive -type inhibitor.

4.3. Molecular docking protocol

Molecular docking (MD) approach was performed using MOE-dock module implemented in the Molecular Operating Environment (MOE) software package [26] to dock all the synthetic derivatives against the α-glucosidase enzyme. We used the homology model described by Guerreiro et al. [27] due to the unavailability of the crystallographic structure yet. Later, the model was subjected for 3D protonation, and the energy was minimized till 0.05 Gradient using MMFF94s force field implemented in MOE. Next, the 3D structures for all derivatives were built using the Molecular Builder Module implemented in MOE. All the derivatives were set flexible, in order to obtain the minimal energy complex during the MD. Later, the docked complexes were ranked based on the docking scores (S). Finally, the predicted ligand-protein complexes were analyzed for molecular interactions using PyMol v1.7.

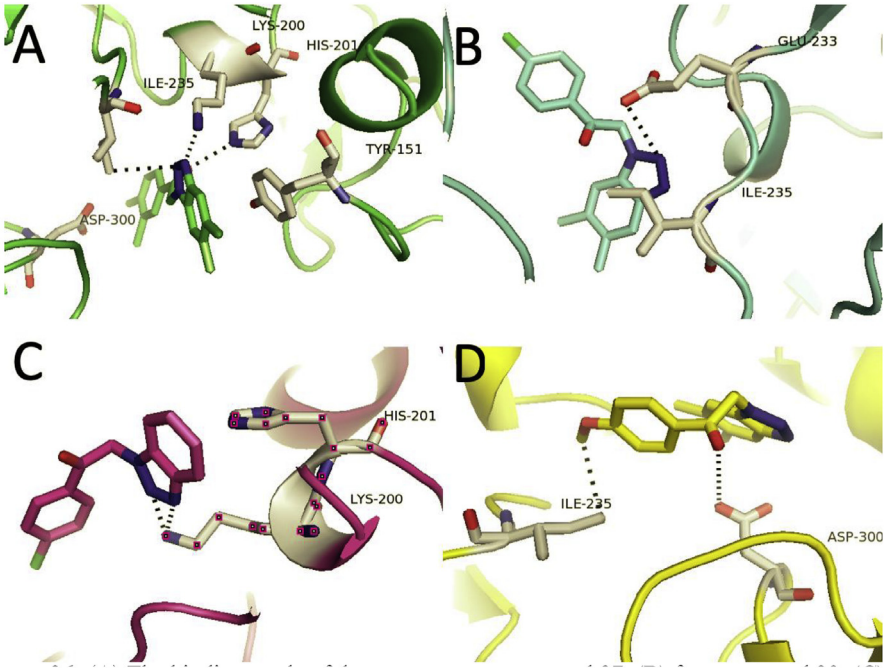

Fig. 26. (**A**) The binding mode of the most potent compound **37**, **(B)** for compound **29**, **(C)** for compound **23**, and **(D)** for compound-**31**.

4.4. Spectral data of synthetic compounds (7–40)

4.4.1. (5,6-Dimethyl-1H-benzo[d][1,2,3] triazol-1-yl)(phenyl) methanone (7) [CAS # 500288-41-5]

Solid: Yield: 62%; M.p.: 142–146 °C; ^{1}H NMR (300 MHz, DMSO-d_6): δ 8.11 (ovp, 3H, H-2′, H-6′, H-1), 8.03 (s, 1H, H-2), 7.78 (t, $J_{4,3/4,5} = 7.5$ Hz, 1H, H-4′), 7.65 (t, $J_{3'(2',4')/5'(4',6')} = 7.8$ Hz, 2H, H-3′, H-5′), 2.47 (s, 3H, CH_3), 2.42 (s, 3H, CH_3), EI-MS *m/z* (% rel. abund.): 251 [M^+, 17], 223 (55), 105 (100), 77 (52), Anal. Calcd for $C_{15}H_{13}N_3O$: C = 71.70; H = 5.21; N = 16.72; O = 6.37; Found: C = 71.65; H = 5.13; N = 16.85; O = 6.35.

4.4.2. (3-Chlorophenyl)(5,6-dichloro-1H-benzo[d][1,2,3] triazol-1-yl)methanone (8)

Solid: Yield: 53%; M.p.: 157–162 °C; ^{1}H NMR (300 MHz, DMSO-d_6): δ 8.79 (s, 1H, H-1, CH), 8.51 (s, 1H, H-4, CH), 8.12 (t, $J_{6',2'/6',4'} = 1.8$ Hz, 1H, H-6′), 8.06 (d, $J_{2',3'} = 7.8$ Hz, 1H, H-2′), 7.87 (dd, $J_{4',3'} = 7.2$ Hz, $J_{4',6'} = 1.2$ Hz, 1H, H-4′), 7.71 (t, $J_{3',2'/3',4'} = 8.1$ Hz, 1H, H-3′); ^{13}C NMR (100 MHz, DMSO-d_6): δc 166.0, 157.1, 144.1, 139.2, 136.6, 133.2, 132.9, 132.6, 130.6, 129.2, 128.7, 127.8, 116.6; EI-MS *m/z* (% rel. abund.): 325 [M^+, 14], 327 (M^++2, 12), 329 (M^++4, 4.2), 297 (52), 139 (100), 111 (50), 75 (23), HREI-MS Calcd for $C_{13}H_6Cl_3N_3O$ *m/z* 324.96 found is 325.96; Anal. Calcd for $C_{13}H_6Cl_3N_3O$: C = 47.81; H = 1.85; Cl = 32.57; N = 12.87; O = 4.90; Found: C = 47.78; H = 1.82; Cl = 32.55; N = 12.85; O = 4.88.

4.4.3. (5,6-Dichloro-1H-benzo[d][1,2,3] triazol-1-yl)(3,4-dimethylphenyl)methanone (9)

Solid: Yield: 52%; M.p.: 143–148 °C; ^{1}H NMR (300 MHz, DMSO-d_6): δ 8.76 (s, 1H, H-1, CH),8.48 (s, 1H, H-2, CH), 7.66 (br. s, 2H, H-2′ H-3′),7.42 (s, 1H, H-6′, CH), 2.38 (s, 6H, CH_3); ^{13}C NMR (100 MHz, DMSO-d_6):δc 166.1, 144.2, 137.7, 135.3, 134.1, 133.8, 131.1, 130.7, 129.3, 128.9, 126.9,121.4, 115.7, 20.7, 20.6; EI-MS *m/z* (% rel. abund.): 319 (M^+, 26), 321 (M^++2, 16), 323 (M^++4, 3), 291 (44), 133 (100), 105 (79), 77 (27); Anal. Calcd for $C_{15}H_{11}Cl_2N_3O$: C = 56.27; H = 3.46; Cl = 22.14; N = 13.12; O = 5.00; Found: C = 56.23; H = 3.43; Cl = 22.10; N = 13.15; O = 4.88.

4.4.4. (5,6-Dichloro-1H-benzo[d][1,2,3]triazol-1-yl)(phenyl) methanone (10) [CAS # 72435-62-2]

Solid: Yield: 72%; M.p.: 160–163 °C; ^{1}H NMR (300 MHz, DMSO-d_6): δ 8.77 (s, 1H, H-1), 8.52 (s, 1H, H-2), 8.12 (d, $J_{2',3'/6',5'} = 7.2$ Hz, 2H, H-2′, H-6′), 7.81 (t, $J_{4',3'/4',5'} = 7.5$ Hz, 1H, H-4′), 7.68 (t, $J_{3'(2',4')/5'(4',6')} = 7.8$ Hz, 2H, H-3′, H-5′), EI-MS *m/z* (% rel. abund.): 291 [M^+, 10], 293 (M^++2, 7),263 (54), 105 (100), 77 (100), 51 (27); Anal. Calcd for $C_{13}H_7Cl_2N_3O$: C = 53.45; H = 2.42; Cl = 24.27; N = 14.38; O = 5.48; Found: C = 53.41; H = 2.39; Cl = 24.24; N = 14.36; O = 5.45.

4.4.5. (1H-Benzo[d][1,2,3]triazol-1-yl)(4-fluorophenyl)methanone (11) [CAS # 203070-37-5]

Solid: Yield: 61%; M.p.: 100–101 °C; ^{1}H NMR (300 MHz, DMSO-d_6): δ 8.35 (t, $J_{2,3/6,5} = 9.0$ Hz, 2H, H-2′, H-6′), 7.95 (ovp, 3H, H-3′, H-5′, H-1), 7.71 (t, $J_{3(2,4)} = 9.0$ Hz, 1H, H-3), 7.52 (ovp = 2H, H-2, H-4), EI-MS *m/z* (% rel. abund.): 241 [M^+, 7], 213 (67), 123 (100), 95 (37); Anal. Calcd for $C_{13}H_8FN_3O$: C = 64.73; H = 3.34; F = 7.88; N = 17.42; O = 6.63; Found: C = 64.71; H = 3.31; F = 7.85; N = 17.40; O = 6.60.

4.4.6. (1H-Benzo[d][1,2,3]triazol-1-yl)(2-chloro-3,4-difluorophenyl)methanone (12)

Solid: Yield: 63%; M.p.: 100–101 °C; ^{1}H NMR (300 MHz, DMSO-d_6): δ 8.35 (ovp, 2H, H-2′, H-3′), 8.22 (ovp, 1H, H-1), 8.08 (dd, $J_{4,3} = 7.2$ Hz, $J_{4,2} = 3.3$ Hz, 1H, H-3), 7.92 (t, $J_{3(2,4)} = 8.1$ Hz, 1H, H-3), 7.73 (t, $J_{2(1,3)} = 8.1$ Hz, 1H, H-2); ^{13}C NMR (75 MHz, DMSO-d_6): δc 165.1, 131.4, 130.5, 127.3, 123.5, 120.4, 119.9, 119.8, 119.6, 119.5, 119.1, 114.4, 113.9; EI-MS *m/z* (% rel. abund.): 293 [M^+, 31], 295 (M^++2, 10), 265 (77), 175 (100), 147 (46); Anal. Calcd for $C_{13}H_6ClF_2N_3O$: C = 53.17; H = 2.06; Cl = 12.07; F = 12.94; O = 5.45; Found: C = 53.14; H = 2.03; Cl = 12.04; F = 12.91; O = 5.42.

4.4.7. (1H-Benzo[d][1,2,3]triazol-1-yl)(2,6-difluorophenyl) methanone (13) [28]

Solid: Yield: 77%; M.p.: 131–133 °C; ^{1}H NMR (300 MHz, DMSO-d_6): δ 8.36 (dd, $J_{1,2/4,3} = 8.1$ Hz, $J_{1,3/4,2} = 3.3$ Hz, 2H, H-1, H-4),

Table 4
Protein Ligand Interaction profile.

S. No	Interaction details						Docking score
	Ligands	Receptor		Distance	E cal/mol	Residue	
7	O 17	NE2	H-acceptor	3.11	−1.5	HIS201	−4.52
	6-ring	CD1	π-H	3.72	−0.7	ILE235	
8	Cl 25	OG1	H-donor	3.30	−1.2	THR163	−5.53
	N 10	NE2	H-acceptor	3.35	−1.0	HIS299	
	O 14	NH2	H-acceptor	3.13	−5.2	ARG195	
	5-ring	6-ring	π-π	4.00	−0.0	TYR62	
9	O 20	CB	H-acceptor	3.45	−0.5	TRP59	−5.58
	6-ring	CD1	π-H	3.82	−0.6	ILE235	
10	N 9	CE	H-acceptor	3.49	−0.5	LYS200	
	6-ring	CE2	π-H	3.52	−0.7	HIS201	−4.47
	5-ring	CD1	π-H	3.61	−0.8	ILE235	
11	N 8	NZ	H-acceptor	3.19	−7.3	LYS200	−5.12
	6-ring	NE2	π-H	3.62	−0.8	HIS201	
	5-ring	CD1	π-H	3.67	−0.8	ILE235	
12	N 9	NH2	H-acceptor	3.75	−2.2	ARG195	−5.23
13	N 8	NZ	H-acceptor	3.23	−8.7	LYS200	
	N 9	CE	H-acceptor	3.51	−0.5	LYS200	−5.09
	6-ring	CE2	π-H	3.57	−0.7	HIS201	
	5-ring	CD1	π-H	3.70	−0.7	ILE235	
14	N 8	O	H-donor	3.69	−0.5	GLN63	
	N 9	O	H-donor	3.12	−1.7	THR163	−5.07
	O 12	O	H-donor	2.72	−2.5	THR163	
15	N 8	NH2	H-acceptor	3.27	−4.8	ARG195	
	N 9	NH2	H-acceptor	3.49	−1.3	ARG195	−4.94
	O 12	NZ	H-acceptor	3.34	−0.6	ALA198	
16	6-ring	CD1	π-H	3.77	−0.5	ILE235	−4.56
17	N 9	NZ	H-acceptor	3.21	−7.8	LYS200	−5.07
18	N 8	NH_2	H-acceptor	3.95	−0.8	ARG195	
	N 9	NE2	H-acceptor	3.47	−0.8	HIS299	−4.95
	O 12	CB	H-acceptor	3.38	−0.5	ALA198	
19	N 8	NH2	H-acceptor	3.67	−0.8	ARG195	−5.72
	N 9	NH2	H-acceptor	3.51	−2.3	ARG195	
20	N 9	NH2	H-acceptor	4.06	−0.5	ARG195	
	O 19	NZ	H-acceptor	3.11	−4.4	LYS200	−5.83
	O 20	CE	H-acceptor	3.59	−0.6	LYS200	
	O 20	N	H-acceptor	3.10	−2.0	ILE235	
21	N 8	NZ	H-acceptor	3.23	−8.7	LYS200	
	N 9	CE	H-acceptor	3.49	−0.5	LYS200	−5.67
	6-ring	CE2	π-H	3.52	−0.7	HIS201	
	5-ring	CD1	π-H	3.61	−0.8	ILE235	
22	N 8	NZ	H-acceptor	3.21	−3.4	LYS200	−4.74
	N 9	NZ	H-acceptor	3.26	−3.0	LYS200	
23	N 8	NH2	H-acceptor	3.48	−1.7	ARG195	−5.86
	N 9	NH2	H-acceptor	3.48	−2.7	ARG195	
24	N 8	NZ	H-acceptor	3.11	−3.5	LYS200	−5.29
	N 9	NZ	H-acceptor	3.32	−0.6	LYS200	
25	N 8	NZ	H-acceptor	3.19	−8.6	LYS200	−5.48
	N 9	CE	H-acceptor	3.49	−0.5	LYS200	
	6-ring	NE2	π-H	3.54	−0.6	HIS201	
26	C 10	OD2	H-donor	3.46	−0.8	ASP300	−5.71
27	C 16	6-ring	H-π	3.58	−0.5	TYR62	
	5-ring	NE2	π-H	3.55	−2.5	HIS201	−6.12
	6-ring	CD1	π-H	3.73	−0.6	ILE235	
28	C 15	6-ring	H-π	4.21	−0.8	TYR62	−5.79
	6-ring	CD1	H-π	3.68	−0.7	ILE235	
29	N 8	NZ	H-acceptor	3.23	−8.7	LYS200	
	N 9	CE	H-acceptor	3.51	−0.5	LYS200	−5.53
	6-ring	NE2	π-H	3.57	−0.7	HIS201	
	5-ring	CD1	π-H	3.70	−0.7	ILE235	
30	C 10	OE1	H-donor	3.52	−0.6	GLU233	
	O 19	OD1	H-donor	2.84	−3.2	ASP197	−5.56
	O 19	CE	H-donor	3.33	−0.6	ASP197	
	5-ring	OD1	π-H	3.70	−1.0	ILE235	
31	5-ring	CD1	π-H	3.75	−0.5	ILE235	−6.02
32	N 8	CB	H-acceptor	3.90	−0.5	ALA198	−5.71
33	5-ring	CD1	pi-H	3.74	−0.6	ILE235	−5.22
34	5-ring	NE2	π-H	3.65	3.65	HIS201	−5.30
35	C6A 6	OE1	H-donor	3.69	−0.5	GLN63	
	O4A 9	O	H-donor	3.12	−1.7	THR163	−5.54
	O6A 11	O	H-donor	2.72	−2.5	THR163	
36	C 10	OE1	H-donor	3.43	−0.6	GLU233	−5.90
	5-ring	CD1	π-H	3.80	−0.8	ILE235	

(*continued on next page*)

Table 4 (*continued*)

S. No	Interaction details						Docking score
	Ligands	Receptor		Distance	E cal/mol	Residue	
37	O	NZ	H-acceptor	3.25	−11.6	LYS200	−5.34
	O	NE2	H-acceptor	3.01	−2.4	HIS201	
	5-ring	CD1	π-H	3.99	−0.5	ILE235	
	6-ring	6-ring	π-π	4.1	−0.5	TYR151	
	6-ring	OD2	π-H	3.9	−0.7	ASP300	
38	C6A 6	OE1	H-donor	3.69	−0.5	GLN63	
	O4A 9	O	H-donor	3.12	−1.7	THR163	−5.90
	O6A 11	O	H-donor	2.72	−2.5	THR163	
39	C6A 6	OE1	H-donor	3.69	−0.5	GLN63	
	C1H	OE1	H-donor	3.02	−3.4	GLU233	−5.56
	C2H	OD1	H-donor	2.90	−1.3	ASP197	
	C3H	OD2	H-donor	3.01	−0.5	ASP300	
40	5-ring	OE1	H-donor	3.02	−0.5	ILE235	
	C2H 34	OD1	H-donor	2.90	−1.3	ASP197	−5.43

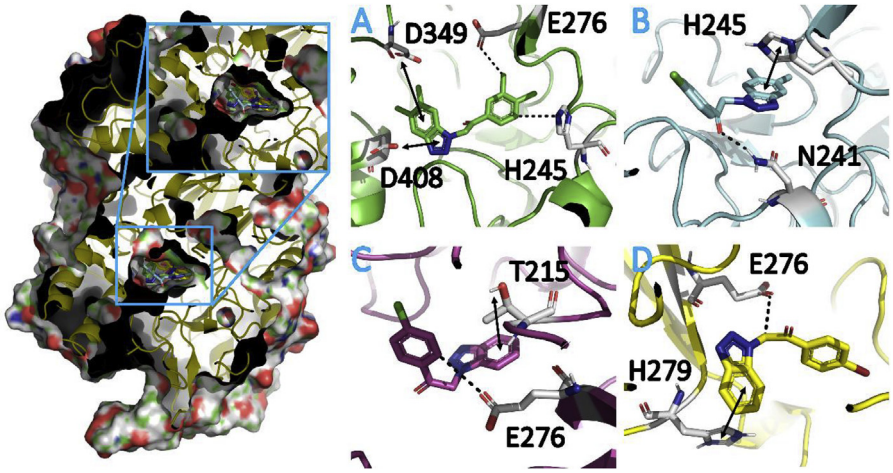

Fig. 27. The ligand-protein interaction (LPI) profile for synthesized derivatives against the α-glucosidase enzyme. The surface representation (left side) of the α-glucosidase enzyme in complex with most active compounds. The double-sided arrow represents pi-stacking interaction. The binding mode of the most potent compound (**A**) for compound **37**, (**B**) compound **36**, (**C**) for compound **25**, and (**D**) for compound **29**.

7.93 (ovp, 2H, H-3, H-4′), 7.74 (t, $J_{2(1,3)}$ = 7.8 Hz, 1H, H-2), 7.46 (t, $J_{5',4'/3',4'}$ = 8.7 Hz, 2H, H-3′, H-5′), EI-MS *m/z* (% rel. abund.): 259 [M^+, 22], 231 (86), 203 (27), 141 (100), 113 (60), 63 (28); Anal. Calcd for $C_{13}H_7F_2N_3O$: C = 60.24; H = 2.72; F = 12.66; N = 16.21; O = 6.17; Found: C = 60.21; H = 2.70; F = 12.63; N = 16.19; O = 6.16.

4.4.8. (1H-Benzo[d][1,2,3]triazol-1-yl)(4-bromophenyl)methanone (14) [29]

Solid; Yield: 81%; M.p.: 138−140 °C; ^{1}H NMR (300 MHz, DMSO-d_6): δ 8.33 (ovp = , 2H, H-1, H-4), 8.06 (d, $J_{2',3'/6',5'}$ = 7.8 Hz, 2H, H-2′, H-6′), 7.68 (ovp, 3H, H-1, H-5′, H-3′), 7.68 ($J_{2(1,3)}$ = 7.8 Hz, 1H, H-2), EI-MS *m/z* (% rel. abund.): 301 (M+ 2, 7.8), 275 (71), 183 (100), 157 (35), 119 (32), 91 (21), 64 (20); Anal. Calcd for $C_{13}H_8BrN_3O$: C = 51.68; H = 2.67; Br = 26.45; N = 13.19; O = 5.30; Found: C = 51.65; H = 2.63; Br = 26.42; N = 13.16; O = 5.28.

4.4.9. (1H-Benzo[d][1,2,3]triazol-1-yl)(4-methoxyphenyl) methanone (15) [CAS # 4231-69-0]

Solid: Yield: 72%; M.p.: 108−111 °C; ^{1}H NMR (300 MHz, DMSO-d_6): δ 8.30 (dd, $J_{2',6'/6',2'}$ = 2.8 Hz, $J_{2'3/6',5'}$ = 8.1 Hz, 2H, H-2′, H-6′), 8.17 (d, $J_{1,2/4,3}$ = 9.0 Hz, 2H, H-1, H-4), 7.83 (t, $J_{3(2,4)}$ = 7.8 Hz, 1H, H-3), 7.66 (t, $J_{2(1,3)}$ = 8.1 Hz, 2H, H-2), 3.90 (s, 3H, OCH_3), EI-MS *m/z* (% rel. abund.): 253 [M^+, 43], 225 (90), 210 (31), 182 (45), 135 (100), 107 (23), 92 (41), 77 (41); Anal. Calcd for $C_{14}H_{11}N_3O_2$: C = 66.40; H = 4.38; N = 16.59; O = 12.63; Found: C = 66.38; H = 4.36; N = 16.56; O = 12.61.

4.4.10. (1H-Benzo[d] [1,2,3]triazol-1-yl)(2-methoxyphenyl) methanone (16) [28]

Solid: Yield: 52%; M.p.: 95−96 °C; ^{1}H NMR (300 MHz, DMSO-d_6), δ 8.30 (ovp, 2H, H-1, H-4), 7.85 (t, $J_{3(2,4)}$ = 7.8 Hz, 1H, H-3), 7.68 (ovp, 3H, H-2, H-4′, H-5′), 7.27 (d, $J_{2',3'}$ = 8.1 Hz, 1H, H-2′), 7.17 (t, $J_{3'(2',4')}$ = 7.5 Hz, 1H, H-3′), 3.71 (s, 3H, OCH_3), EI-MS *m/z* (% rel. abund.): 253 [M^+, 80], 224 (89), 196 (31), 135 (100), 92 (50), 77 (77), 64 (24); Anal. Calcd for $C_{14}H_{11}N_3O_2$: C = 66.40; H = 4.38; N = 16.59; O = 12.63; Found: C = 66.38; H = 4.36; N = 16.56; O = 12.61.

4.4.11. (1H-Benzo[d][1,2,3]triazol-1-yl)(m-tolyl) methanone (17) [29]

Solid: Yield: 69%; M.p.: 65−67 °C; ^{1}H NMR (300 MHz, DMSO-d_6): δ 8.31 (ovp, 2H, H-1, H-4), 7.90 (ovp, 2H, H-6′, H-2′), 8.85 (t, $J_{3(2,4)}$ = 7.8 Hz, 1H, H-3), 7.67 (ovp, 3H, H-3′, H-4′, H-2), 2,40 (s, 3H, CH_3), EI-MS *m/z* (% rel. abund.): 237 [M^+, 7], 209 (55), 119 (100), 91 (58); Anal. Calcd for $C_{14}H_{11}N_3O$: C = 70.87; H = 4.67; N = 17.71; O = 6.74: Found: C, 70.85; H, 4.65; N, 17.69; O = 6.72.

Table 5
Interaction detail for all derivatives against α-glucosidase enzyme.

S. No	Interaction details						Docking score
	Ligands	Receptor		Distance	E cal/mol	Residue	
7	C 14	5-ring	H-π	3.90	−0.7	HIS245	−5.70
8	5-ring	CE1	π-H	4.18	−0.6	PHE177	−5.89
9	CL 19	O	H-donor	3.74	−1.0	LEU437	−6.36
10	O 17	NH2	H-acceptor	2.87	−4.1	ARG212	−5.87
11	C 15	5-ring	H-π	3.80	−0.8	HIS245	−6.31
12	CL 18	OE2	H-donor	3.30	−1.2	GLU304	−5.46
	C 1	5-ring	H-π	3.85	−0.6	HIS245	
13	C 13	5-ring	H-π	3.93	−1.0	PHE157	−5.42
14	O 12	ND2	H-acceptor	3.47	−1.0	ASN241	−5.90
15	C 1	5-ring	H-π	4.08	−0.6	HIS245	−5.82
16	5-ring	CD2	π-H	3.52	−1.7	HIS279	−5.70
	5-ring	CD2	π-H	3.91	−0.9	HIS279	
17	C 1	5-ring	H-π	3.61	−0.5	HIS245	−5.93
18	6-ring	CG2	πH	4.08	−0.8	THR215	−5.93
19	C 6	5-ring	H-π	3.71	−0.6	HIS245	−6.06
20	C 14	5-ring	H-π	3.59	−0.8	HIS245	−5.96
	6-ring	CD2	π-H	4.62	−0.6	HIS279	
21	O 21	NH2	H-acceptor	3.10	−2.4	ARG212	−6.200
	6-ring	CD2	π-H	4.61	−0.8	HIS279	
22	N 19	6-ring	H-π	3.37	−0.5	PHE300	−5.73
23	N 9	NH1	H-acceptor	3.07	−0.5	ARG439	−6.64
	C 15	6-ring	H-π	3.96	−0.6	PHE157	
	6-ring	CG2	π-H	4.22	−0.7	THR215	
24	C 17	OD2	H-donor	3.35	−0.5	ASP349	−5.37
	N 8	NH2	H-acceptor	3.12	−0.8	ARG212	
25	6-ring	CG2	π-H	4.08	−0.8	THR215	−6.095
	C 18	OE1	H-donor	3.34	−0.8	GLU276	
26	CL 19	O	H-donor	3.89	−0.7	PRO309	−5.98
27	C 10	OE1	H-donor	3.43	−0.5	GLU276	−6.33
	C 1	5-ring	H-π	3.88	−0.5	HIS245	
28	C 1	5-ring	H-π	3.88	−0.5	HIS245	−6.20
29	6-ring	CD2	π-H	4.44	−0.7	HIS279	−5.99
	C 18	OE1	H-donor	3.34	−0.9	GLU276	
30	C 10	OE1	H-donor	3.18	−1.3	GLU276	−5.98
	O 13	NH2	H-acceptor	3.08	−2.3	ARG212	
	O 19	NE2	H-acceptor	3.08	−0.9	HIS348	
31	C 10	OE1	H-donor	3.33	−0.5	GLU276	−6.22
	C 18	OE1	H-donor	3.34	−0.8	GLU276	
	6-ring	CD2	π-H	4.44	−0.7	HIS279	
32	C 10	OE1	H-donor	3.66	−0.5	GLU276	−6.06
	C 1	5-ring	H-π	3.76	−1.1	HIS245	
33	C 10	OE1	H-donor	3.57	−0.6	GLU276	−6.14
	5-ring	CE1	π-H	4.13	−0.6	PHE177	
	6-ring	CG2	π-H	4.09	−0.5	THR215	
34	6-ring	NH2	π-cation	4.59	−0.5	ARG212	−5.62
35	5-ring	CD2	π-H	4.08	−1.0	HIS279	−6.81
36	O 13	CD2	H-acceptor	3.19	−1.2	ASN241	−6.41
	5-ring	ND2	π-H	3.78	−0.7	HIS245	
37	CL 22	OE1	H-donor	3.52	−0.7	GLU276	−6.42
	C 17	5-ring	h-donor	4.08	−0.6	HIS245	
	C 17	5-ring	H-π	3.02	−3.9	ASP408	
	C 5	6-ring	πi-π	2.8	−0.5	ASP349	
38	O 21	OD2	H-donor	3.02	−3.9	ASP408	−6.46
	6-ring	CD	π-H	3.72	−0.5	ARG439	
39	6-ring	CG2	π-H	4.08	−0.8	THR215	−6.06
40	5-ring	CD2	π-H	3.92	−1.7	HIS279	−6.64

4.4.12. (1H-Benzo[d][1,2,3]triazol-1-yl)(3,4-dimethylphenyl) methanone (18) [CAS # 333348-56-4]

Solid: Yield: 63%; M.p.: 95-94 °C; ^{1}H NMR (300 MHz, DMSO-d_6), δ 8.30 (dd, $J_{1,2/4,3} = 8.4$ Hz, $J_{1,3/4,2} = 3.0$ Hz, 2H, H-1, H-4), 7.84 (t, $J_{3(2,4)} = 7.5$ Hz, 1H, H-3), 7.69 (ovp, 3H, H-2, H-5′, H-6′), 7.41 (s, 1H, H-2′), 2.38 (s, 6H, CH_3), EI-MS *m/z* (% rel. abund.): 251 [M^+, 56], 223 (91), 208 (38), 133 (100), 105 (82), 77 (42); Anal. Calcd for $C_{15}H_{13}N_3O$: C = 71.70; H = 5.21; N = 16.72; O = 6.37; Found: C = 71.68; H = 5.20; N = 16.70; O = 6.36.

4.4.13. (1H-Benzo[d][1,2,3]triazol-1-yl)(3,4,5-trimethylphenyl) methanone (19)

Solid: Yield: 81%; M.p.: 118−119 °C; ^{1}H NMR (300 MHz, DMSO-d_6): δ 8.29 (d, $J_{1,2/4,3} = 8.4$ Hz, 2H, H-1, H-4),7.85 (t, $J_{3(2,4)} = 7.5$ Hz, 1H, H-3), 7.65 (t, $J_{2(1,3)} = 7.8$ Hz, 1H, H-2), 7.46 (s, 2H, H-2′, H-6′); ^{13}C NMR (75 MHz, DMSO-d_6):δc 166.8, 152.5, 152.4, 131.8, 130.6, 126.5, 126.1, 120.7, 114.5, 114.2, 109.3, 106., 60.2, 60.0, 56.2, 55.8; EI-MS *m/z* (% rel. abund.): 265 [M^+, 29], 240 (60), 210 (17), 194 (39), 150 (100), 104 (56), 76 (33); Anal. Calcd for $C_{16}H_{15}N_3O$: C = 72.43; H = 5.70; N = 15.84; O = 6.03; Found:

C = 71.68; H = 5.20; N = 16.70; O = 6.36.

4.4.14. (1H-Benzo[d][1,2,3]triazol-1-yl)(4-nitrophenyl)methanone (20) [30]

Solid: Yield: 74%; M.p.: 188–193 °C; ^{1}H NMR (300 MHz, DMSO-d_6): δ 8.46 (d, $J_{2'3'/6',5'}$ = 8.7 Hz, 2H, H-2′, H-6′), 8.48 (ovp, 4H, H-3′, H-5′, H-1, H-4), 7.88 (t, $J_{3(2,4)}$ = 7.5 Hz, 1H, H-3), 7.70 (t, $J_{2(1,3)}$ = 7.8 Hz, 1H, H-2), EI-MS *m/z* (% rel. abund.): 268 [M$^+$, 29], 240 (60), 210 (17), 194 (39), 150 (100), 104 (56), 76 (33); Anal. Calcd for $C_{13}H_8N_4O_3$: C = 58.21; H = 3.01; N = 20.89; O = 17.89; Found: C = 58.18; H = 3.00; N = 20.84; O = 17.86.

4.4.15. (1H-Benzo[d][1,2,3] triazol-1-yl)(3-methyl-4-nitrophenyl) methanone (21) [CAS # 328555-26-6]

Solid: Yield: 67%; M.p.: 109–112 °C; ^{1}H NMR (300 MHz, DMSO-d_6): δ 8.35 (t, $J_{1,2/4,3}$ = 8.4 Hz, 2H, H-1, H-4),8.20 (ovp, 3H, H-2′, H-5′, H-6′), 7.88 (t, $J_{3(2,4)}$ = 7.2 Hz, 1H, H-3), 7.70 (t, $J_{2(1,3)}$ = 7.8 Hz, 1H, H-2), 2.60 (s, 3H, CH_3), EI-MS *m/z* (% rel. abund.): 282 [M$^+$, 24], 254 (19), 237 (22), 164 (100), 118 (38), 106 (26) 89 (24); Anal. Calcd for $C_{13}H_8N_4O_3$: C = 59.57; H = 3.57; N = 19.85; O = 17.00; Found: C = 59.56; H = 3.55; N = 19.83; O = 16.98.

4.4.16. (3-Amino-4-chlorophenyl)(1H-benzo[d][1,2,3] triazol-1-yl) methanone (22)

Solid: Yield: 58%; M.p.: 133–144 °C; ^{1}H NMR (300 MHz, DMSO-d_6): δ 8.30 (d, $J_{1,2/4,3}$ = 9.0 Hz, 2H, H-1, H-4), 7.84 (t, $J_{3(2,4)}$ = 7.8 Hz, 1H, H-3), 7.86 (t, $J_{2(1,3)}$ = 8.4 Hz, 1H, H-2), 7.54 (d, $J_{5',2'}$ = 1.8 Hz, 1H, H-5′), 7.46 (d, $J_{3',2'}$ = 8.1 Hz, 1H, H-3′), 7.28 (dd, $J_{2',5'}$ = 1.8 Hz, $J_{2',3'}$ = 6.3 Hz, 1H, H-2′), 5.80 (s, 2H, NH_2); ^{13}C NMR (100 MHz, DMSO-d_6):δc 166.0, 145.1, 144.7, 131.7, 130.6, 130.6, 129.0, 126.6, 122.2, 119.9, 119.4, 117.5, 114.4; EI-MS *m/z* (% rel. abund.): 272 [M$^+$, 83], 274 (M$^+$+2, 25), 244 (34), 156 (51), 154 (100), 126 (43), 90 (39); Anal. Calcd for $C_{13}H_9ClN_4O$: C = 57.26; H = 3.33; Cl = 13.00; N = 20.55; O = 5.87; Found: C = 57.23; H = 3.31; Cl = 12.98; N = 20.53; O = 5.85.

4.4.17. (1H-Benzo[d][1,2,3]triazol-1-yl)(4-butoxyphenyl) methanone (23) [CAS # 574711-93-6]

Solid: Yield: 80%; M.p.: 126–137 °C; ^{1}H NMR (300 MHz, DMSO-d_6), δ 8.24 (d $J_{2'3'/6',5'}$ = 7.8 Hz, 2H, H-2′, H-6′), 8.18 (d, $J_{1,2}$ = 8.1 Hz, 1H, H-1), 8.16 (d, $J_{3',2'}$ = 8.7 Hz, 1H, H-3′), 7.82 (t, $J_{3(2,4)}$ = 7.2 Hz, 1H, H-3), 7.65 (t, $J_{2(1,3)}$ = 7.8 Hz, 1H, H-2), 7.18 (d, $J_{5',6'}$ = 8.7 Hz, 1H, H-5′), 7.13 (d, $J_{4,3}$ = 9.0 Hz, 1H, H-4), 4.14 (ovp, 2H, CH_2), 1.79 (ovp, 2H, CH_2), 1.51 (ovp, 2H, CH_2), 0.96 (ovp, 3H, CH_3), EI-MS *m/z* (% rel. abund.): 295 [M$^+$, 22], 211 (42), 177 (100), 121 (88); Anal. Calcd for $C_{17}H_{17}N_3O_2$: C = 69.14; H = 5.80; N = 14.23; O = 10.83; Found: C = 69.12; H = 5.77; N = 14.21; O = 10.81.

4.4.18. (1H-Benzo[d][1,2,3]triazol-1-yl)(phenyl)methanone (24) [28]

Solid; Yield: 63%; M.p.: 102–104 °C; ^{1}H NMR (300 MHz, DMSO-d_6), δ 8.34 (ovp, 2H, H-1, H-4), 8.12 (d, $J_{2',3/6',5'}$ = 7.5 Hz, 2H, H-2′, H-6′), 7.86 (t, $J_{3(2,4)}$ = 7.8 Hz, 1H, H-3), 7.79 (t, $J_{2(1,3)}$ = 7.5 Hz, 1H, H-2), 7.68 (ovp, 3H, H-3′, H-4′, H-5′), EI-MS *m/z* (% rel. abund.): 223 [M$^+$, 24], 195 (100), 167 (44), 105 (100), 77 (89), 51 (38); Anal. Calcd for $C_{13}H_9N_3O$: C = 69.95; H = 4.06; N = 18.82; O = 7.17; Found: C = 69.92; H = 4.03; N = 18.80; O = 7.15.

4.4.19. 2-(1H-Benzo[d][1,2,3]triazol-1-yl)-1-(4-chlorophenyl) ethan-1-one (25) [31]

Solid: Yield: 55%; M.p.: 150–152 °C; ^{1}H NMR (300 MHz, DMSO-d_6), δ 8.15 (d, $J_{2',3'/6',5'}$ = 8.7 Hz, 2H, H-2′, H-6′), 8.09 (d, $J_{4,3}$ = 8.1 Hz, 1H, H-4), 7.81 (d, $J_{1,2}$ = 8.4 Hz, 1H, H-1), 7.73 (d, $J_{3',2/5',6'}$ = 8.4 Hz, 2H, H-3′, H-5′), 7.55 (t, $J_{3(2,4)}$ = 7.8 Hz, 1H, H-3), 7.44 (t, $J_{2(1,3)}$ = 7.8 Hz, 1H, H-2), 6.57 (s, 2H, CH_2), EI-MS *m/z* (% rel. abund.): 271 [M$^+$, 16], 273 (M$^+$+2, 6), 140 (38), 138 (93), 132 (100), 110 (40), 104 (57),77 (86); Anal. Calcd for $C_{14}H_{10}ClN_3O$: C = 61.89; H = 3.71; Cl = 13.05; N = 15.47; O = 5.89; Found: C = 61.88; H = 3.69; Cl = 13.03; N = 15.44; O = 5.86.

4.4.20. 2-(1H-Benzo[d][1,2,3]triazol-1-yl)-1-(3,4-dichlorophenyl) ethan-1-one (26) [CAS #1456055-61-0]

Solid: Yield: 76%; M.p.: 179–181 °C; ^{1}H NMR (300 MHz, DMSO-d_6), δ 8.37 (d, $J_{6',2'}$ = 1.8 Hz, 1H, H-6′), 8.09 (dd, $J_{2',3'/3',2'}$ = 8.4 Hz, $J_{2',6'}$ = 3.6 Hz, 2H, H-2′, H-3′), 7.93 (d, $J_{4,3}$ = 8.4 Hz, 1H, H-4), 7.80 (d, $J_{1,2}$ = 8.4 Hz, 1H, H-1), 7.55 (t, $J_{3(2,4)}$ = 7.5 Hz, 1H, H-3), 7.44 (t, $J_{2(1,3)}$ = 7.8 Hz, 1H, H-2), 6.59 (s, 2H, CH_2), EI-MS *m/z* (% rel. abund.): 305 [M$^+$, 14], 307 (M$^+$+2, 9), 248 (24), 144 (54), 132 (100), 104 (70), 77 (80); Anal. Calcd for $C_{14}H_9Cl_2N_3O$: C = 54.93; H = 2.96; Cl = 23.16; N = 13.73; O = 5.23; Found: C = 54.91; H = 2.94; Cl = 23.14; N = 13.71; O = 5.21.

4.4.21. 2-(1H-Benzo[d] [1–3]triazol-1-yl)-1-(2,3-dichlorophenyl) ethan-1-one (27)

Solid: Yield: 60%; M.p.: 144–146 °C; ^{1}H NMR (300 MHz, DMSO-d_6), δ 8.16 (dd, $J_{1,2/4,3}$ = 8.4 Hz, 2H, H-1, H-4), 7.84 (ovp, 2H, H-5′, H-6′), 7.71 (d, $J_{4',6'}$ = 1.8 Hz, $J_{4',5'}$ = 8.4 Hz, 1H, H-4′), 7.58 (t, $J_{3(2,4)}$ = 7.8 Hz, 1H, H-3), 7.45 (t, $J_{2(1,3)}$ = 7.5 Hz, 1H, H-2), 6.44 (s, 2H, CH_2); ^{13}C NMR (75 MHz, DMSO-d_6):δc 193.1, 145.0, 137.4, 133.7, 133.4, 132.1, 131.6, 130.5, 127.6, 127.5, 123.9,119.1, 110.8, 56.02; EI-MS *m/z* (% rel. abund.): 305 [M$^+$, 3], 307 (M$^+$+2, 2),132 (100), 104 (35), 77 (63), HREI-MS Calcd for $C_{14}H_9Cl_2N_3O$ *m/z* 305.0117, Found: 305.0128; Anal. Calcd for $C_{14}H_9Cl_2N_3O$: C = 54.93; H = 2.96; Cl = 23.16; N = 13.73; O = 5.23; Found: C = 54.90; H = 2.93; Cl = 23.12; N = 13.69; O = 5.20.

4.4.22. 2-(1H-Benzo[d][1,2,3]triazol-1-yl)-1-(3-bromophenyl) ethan-1-one (28) [CAS # 1455104-78-5]

Solid: Yield: 75%; M.p.: 126–128 °C; ^{1}H NMR (300 MHz, DMSO-d_6): δ 8.29 (s, 1H, H-2′), 8.11 (t, $J_{6',5'/4',5'}$ = 7.5 Hz, 2H, H-6′, H-4′), 7.97 (d, $J_{4,3}$ = 7.8 Hz, 1H, H-4), $J_{1,4}$ = 8.1 Hz, 1H, H-1),7.62(t, $J_{3(2,4)}$ = 7.8 Hz, 1H, H-3), 7.55 (t, $J_{2(1,3)}$ = 7.8 Hz, 1H, H-2), 7.44 (t, $J_{5',4'/5',6'}$ = 7.8 Hz, 1H, H-5′), 6.59 (s, 2H, CH_2), EI-MS *m/z* (% rel. abund.): 315 [M$^+$, 7], 317 (M$^+$+2, 7),183 (3), 132 (100), 104 (33), 77 (47); Anal. Calcd for $C_{14}H_{10}BrN_3O$: C = 53.19; H = 3.19; Br = 25.27; N = 13.29; O = 5.06; Found: C = 53.17; H = 3.17; Br = 25.25; N = 13.27; O = 5.04.

4.4.23. 2-(1H-Benzo[d][1,2,3]triazol-1-yl)-1-(4-bromophenyl) ethan-1-one (29) [30]

Solid: Yield: 65%; M.p.: 160–196 °C; ^{1}H NMR (300 MHz, DMSO-d_6): δ 8.09 (d, $J_{4,3}$ = 6.9 Hz, 1H, H-4), 8.06 (dd, $J_{2',3'/6',5'}$ = 6.9 Hz, 2H, H-2′, H-6′), 7.84 (d, $J_{3',2'/5',6'}$ = 8.4 Hz, 2H, H-3′, H-5′), 7.80 (d, $J_{1,2}$ = 8.4 Hz, 1H, H-1),7.55 (t, $J_{3(2,4)}$ = 7.5 Hz, 1H, H-3),7.44 (t, $J_{2(1,3)}$ = 7.8 Hz, 1H, H-2), 6.57 (s, 2H, CH_2), EI-MS *m/z* (% rel. abund.): 315 [M$^+$, 9], 317 (M$^+$ +2, 9), 132 (100), 104 (50), 77 (81); Anal. Calcd for $C_{14}H_{10}BrN_3O$: C = 53.19; H = 3.19; Br = 25.27; N = 13.29; O = 5.06; Found: C = 53.17; H = 3.17; Br = 25.25; N = 13.27; O = 5.04.

4.4.24. 2-(1H-Benzo[d][1,2,3]triazol-1-yl)-1-(2-hydroxyphenyl) ethan-1-one (30)

Solid: Yield: 60%; M.p.: 160–165 °C; ^{1}H NMR (300 MHz, DMSO-d_6): δ 11.21 (s, 1H, OH), 8.08 (d, J = 8.4 Hz, 1H, H-4), 7.88 (dd, $J_{6',5'}$ = 6.6 Hz, $J_{6',4'}$ = 1.5 Hz, H-6′), 7.81 (d, $J_{1,2}$ = 8.4 Hz, 1H, H-1), 7.59 (ovp, 2H, H-5′, H-3), 7.43 (t, $J_{2(1,3)}$ = 7.8 Hz, 1H, H-2), 7.10 (d, $J_{3',4'}$ = 8.4 Hz, 1H, H-3′), 7.02 (t, $J_{4'(3',5')}$ = 7.4 Hz, 1H, H-4′), 7.02 (t, $J_{3',5'}$ = 7.5 Hz, 1H, H-4′), 6.39 (s, 2H, CH_2); ^{13}C NMR (75 MHz, DMSO):δc 193.9, 159.6, 145.0, 136.0, 133.9, 130.2, 127.2, 123.7, 120.6, 119.4, 118.9,117.6, 111.0, 56.4; EI-MS *m/z* (% rel. abund.): 253 [M$^+$,

44], 225 (26), 132 (38), 121 (100), 104 (36), 93 (23), 77 (71), HREI-MS *m/z* Calcd for $C_{14}H_{11}N_3O_2$ 253.0851 Found 253.0850; Anal. Calcd for $C_{14}H_{11}N_3O_2$: C = 66.40; H = 4.38; N = 16.59; O = 12.63; Found: C = 66.36; H = 4.36; N = 16.55; O = 12.60.

4.4.25. 2-(1H-Benzo[d][1,2,3]triazol-1-yl)-1-(3-nitrophenyl)ethan-1-one (31) [30]

Solid: Yield: 71%; M.p.: 173–177 °C; ^{1}H NMR (300 MHz, DMSO-d_6): δ 8.84 (s,1H, H-2′), 7.59 (dd, $J_{4',5'/6',5'}$ = 7.8 Hz, 2H, H-4′, H-6′), 8.10 (d, $J_{3(2,4)}$ = 8.4 Hz, 1H, H-1), 7.96 (t, $J_{5',4'/5',6'}$ = 8.1 Hz, 1H, H-5′), 7.84 (d, $J_{1,2}$ = 8.1 Hz, 1H, H-1), 7.56 (t, $J_{3(2,4)}$ = 7.8 Hz, 1H, H-3), 7.45 (t, $J_{2(1,3)}$ = 7.8 Hz, 1H, 2), 6.70 (s, 2H, CH_2), EI-MS *m/z* (% rel. abund.): 282 [M^+, 6], 150 (24), 132 (100), 104 (37), 77 (53); Anal. Calcd for $C_{14}H_{10}N_4O_3$: C = 59.57; H = 3.57; N = 19.85; O = 17.00; Found: C = 59.55; H = 3.56; N = 19.83; O = 16.98.

4.4.26. 2-(1H-Benzo[d][1,2,3]triazol-1-yl)-1-(4-methoxyphenyl) ethan-1-one (32) [30]

Solid: Yield: 60%; M.p.: 135–136 °C; ^{1}H NMR (300 MHz, DMSO-d_6): δ 8.11 (ovp, 3H, H-2′, H-6′, H-4), 7.77 (d, $J_{4,3}$ = 8.1 Hz, 1H, H-4), 7.54 (t, $J_{3(2,4)}$ = 8.1 Hz, 1H, H-3),7.43 (t, $J_{2(1,3)}$ = 7.5 Hz, 1H, H-2), 7.16 (d, $J_{3',2'/5',6'}$ = 8.7 Hz, 2H, H-3′, H-5′), 6.49 (s, 2H, CH_2), 3.88(s, 3H, OCH_3), EI-MS *m/z* (% rel. abund.): 267 [M^+, 25], 135 (100), 107 (32), 92 (28), 77 (80); Anal. Calcd for $C_{15}H_{13}N_3O_2$: C = 67.40; H = 4.90; N = 15.72; O = 11.97; Found: C = 67.38; H = 4.88; N = 15.70; O = 11.95.

4.4.27. 2-(1H-Benzo[d][1,2,3]triazol-1-yl)-1-(p-tolyl)ethan-1-one (33) [31]

Solid: Yield: 70%; M.p.: 134–146 °C; ^{1}H NMR (300 MHz, DMSO-d_6): δ 8.13 (d $J_{1,3}$ = 9.0 Hz, 1H, H-1), 8.04 (d, $J_{2',3'/6',5'}$ = 6.0 Hz, 2H, H-2′, H-6′), 7.79(d, $J_{4,3}$ = 9.0 Hz, 1H, H-4), 7.56 (t, $J_{3\ (2,4)}$ = 9.0 Hz, 1H, H-3), 7.45 (t, $J_{3',2'/5',6'}$ = 9 Hz, 2H, H-3′, H-5′), 7.45 (ovp, 1H, H-2), 6.53 (s, 2H, CH_2), 2.43 (s, 3H, CH_3), EI-MS *m/z* (% rel. abund.): 251 [M^+, 14], 132 (29), 119 (100), 104 (26), 91 (70), 77 (63); Anal. Calcd for $C_{15}H_{13}N_3O$: C = 71.70; H = 5.21; N = 16.72; O = 6.37; Found: C = 71.68; H = 5.19; N = 16.70; O = 6.35.

4.4.28. 2-(5,6-Dimethyl-1H-benzo[d][1,2,3]triazol-1-yl)-1-(4-methoxyphenyl)ethan-1-one (34) [CAS # 127876-36-2]

Solid: Yield: 87%; M.p.: 111–114 °C; ^{1}H NMR (300 MHz, DMSO-d_6): δ 8.14 (d, $J_{2,3/6,5}$ = 7.5 Hz, 2H, H-2′, H-6′), 8.09 (d, $J_{1,2}$ = 8.4 Hz, 1H, H-1), 7.81 (ovp, 2H, H-4′, H-4),7.65 (t, $J_{3'(2',4')/5'\ (4',6')}$ = 7.5 Hz, 2H, H-3′, H-5′), 7.55 (t, $J_{3\ (2,4)}$ = 7.8 Hz, H-3), 7.44 (t, $J_{2(1,2)}$ = 7.8 Hz, H-2), 6.57 (s, 2H, CH_2), EI-MS *m/z* (% rel. abund.): 237, [M^+, 23], 209 (19), 180 (25), 132 (42), 105 (5), 77 (4); Anal. Calcd for $C_{14}H_{11}N_3O$: C = 70.87; H = 4.67; N = 17.71; O = 6.74; Found: C = 70.85; H = 4.64; N = 17.69; O = 6.72.

4.4.29. 1-([1,1′-Biphenyl]-4-yl)-2-(1H-benzo[d][1,2,3]triazol-1-yl) ethan-1-one (35) [31]

Solid: Yield: 73%; M.p.: 149–155 °C; ^{1}H NMR (300 MHz, DMSO-d_6): δ 8.23 (d, $J_{2',3'/6',5'}$ = 8.4 Hz, 2H, H-2′, H-6′), 8.10 (d, $J_{4,3}$ = 8.1 Hz, 1H, H-4), 7.95 (d, $J_{3',4'/5',6'}$ = 8.4 Hz, 2H, H-3′, H-5′), 7.82 (ovp = 3H, H-2″, H-6″, H-1), 7.56 ($J_{3''\ (2'',4'')/5''\ (6'',4'')/4''\ (3'',5'')}$ = 8.1 Hz, 3H, H-3″, H-5″, H-4″), 7.45 (t, $J_{2(1,3)/3(2,4)}$ = 7.8 Hz, 2H, H-2, H-3), 6.60 (s, 2H, CH_2), EI-MS *m/z* (% rel. abund.): 313 [M^+, 5], 181 (100), 152 (28), 77 (17); Anal. Calcd for $C_{20}H_{15}N_3O$: C = 76.66; H = 4.83; N = 13.41; O = 5.11; Found: C = 76.64; H = 4.80; N = 13.39; O = 5.10.

4.4.30. 1-(4-Chlorophenyl)-2-(5,6-dimethyl-1H-benzo[d][1,2,3] triazol-1-yl)ethan-1-one (36) [CAS #1902036-34-3]

Solid: Yield: 70%; M.p.: 177–191 °C; ^{1}H NMR (300 MHz, DMSO-d_6) δ 8.14 (d, $J_{2',3'/6',5'}$ = 8.4 Hz, 2H, H-2′ H-6′), 7.80 (s, 1H, H-2), 7.72 (d, $J_{3',2'/5',6'}$ = 8.4 Hz, 2H, H-3′, H-5′), 7.54 (s, 1H, H-1), 6.47 (s, 2H, CH_2), 2.36 (s, 3H, H-2″, CH_3), 2.36 (s, 3H, H-1″, CH_3), EI-MS *m/z* (% rel. abund.): 299 [M^+, 6], 301 (M^++2, 2), 242 (13), 160 (100), 139 (46), 132 (96), 105 (41); Anal. Calcd for $C_{16}H_{14}ClN_3O$: C = 64.11; H = 4.71; Cl = 11.83; N = 14.04; O = 5.34; Found: C = 64.09; H = 4.69; Cl = 11.81; N = 14.02; O = 5.32.

4.4.31. 1-(3,4-Dichlorophenyl)-2-(5,6-dimethyl-1H-benzo[d] [1–3] triazol-1-yl)ethan-1-one (37)

Solid: Yield: 70%; M.p.: 190–196 °C; ^{1}H NMR (300 MHz, DMSO-d_6), δ 8.36 (d, $J_{6',2'}$ = 1.8 Hz, 1H, H-6′), 8.06 (dd, $J_{2',3'}$ = 1.8 Hz, $J_{2',6'}$ = 6.6 Hz, H-2′), 7.93 (d, $J_{2',3'}$ = 8.4 Hz, 1H, H-3′), 7.81 (s, 1H, H-2), 7.54 (s, 1H, H-1), 6.49 (s, 2H, CH_2), 2.36 (s, 3H, H-2″, CH_3), 2.34 (s, 3H, H-1″, CH_3); ^{13}C NMR (75 MHz, DMSO):δc 190.8, 144.3, 137.3, 136.9, 134.4, 132.8, 131.9, 131.2, 130.8, 128.2, 118.1, 109.9, 54.1, 20.3, 19.8; EI-MS *m/z* (% rel. abund.): 333 [M^+, 4], 335 (M^+ +2, 2), 305 (23), 276 (28), 173 (66), 160 (81), 132 (100), 105 (68), 77 (26), HREI-MS *m/z*: Calcd for $C_{16}H_{13}Cl_2N_3O$ 333.0436, Found: 333.0445; Anal. Calcd for $C_{16}H_{13}Cl_2N_3O$: C = 53.50; H = 4.92; Cl = 22.21; N = 11.57; O = 4.79; Found: C = 53.30; H = 4.88; Cl = 22.16; N = 11.51; O = 4.73.

4.4.32. 2-(5,6-Dimethyl-1H-benzo[d][1,2,3]triazol-1-yl)-1-(2-hydroxyphenyl)ethan-1-one (38)

Solid: Yield: 72%; M.p.: 177–179 °C; ^{1}H NMR (300 MHz, DMSO-d_6), 7.89 (d, $J_{6',5'}$ = 6.9 Hz, 1H, H-6′), 7.80 (s, 1H, H-2), 7.58(t, $J_{5',4'/5',6'}$ = 9.6 Hz, 1H, 5′-H), 7.53 (br.s, 1H, H-1), 7.08 (d, $J_{3',4'}$ = 8.1 Hz, 1H, H-3′), 7.02 (t, $J_{4',3'/4',5'}$ = 7.5 Hz, 1H, H-4′), 6.30 (s, 2H, CH_2), 2.36 (s, 3H, H-2″, CH_3), 2.36 (s, 3H, H-1″, CH_3); ^{13}C NMR (75 MHz, DMSO):δc 194.2, 159.6, 144.3, 137.1, 136.0, 133.1, 132.9, 130.2, 120.4, 119.4, 117.9,117.5, 110.0, 56.0, 20.2, 19.8; EI-MS *m/z* (% rel.abund.): 281 [M^+, 54], 253 (21), 160 (55), 132 (100), 121 (77),105 (33); HREI-MS calcd for $C_{16}H_{15}N_3O_2$ *m/z* 281.1164 Found: 281.1161; Anal. Calcd for $C_{16}H_{15}N_3O_2$: C = 65.31; H = 6.37; N = 13.94; O = 10.37; Found: C = 65.25; H = 6.33; N = 13.89; O = 10.35.

4.4.33. 2-(5,6-Dimethyl-1H-benzo[d][1,2,3]triazol-1-yl)-1-phenylethan-1-one (39) [CAS #1907374-75-7]

Solid: Yield: 59%; M.p.: 149–151 °C; ^{1}H NMR (300 MHz, DMSO-d_6), δ 8.13 (d, $J_{2',3'/6',5'}$ = 7.5 Hz, 2H, H-2′, H-4′), 7.81 (s, 1H, H-2), 7.77 (t, $J_{4'\ (3',5')}$ = 7.5 Hz, 1H, H-4′), 7.65 (t, $J_{3'\ (2'3')/5'\ (6',4)}$ = 7.5 Hz, 2H, H-3′, H-5′), 7.54 (s, 1H, H-1), 6.47 (s, 2H, CH_2), EI-MS *m/z* (% rel.abund.): 265 [M^+, 4], 208 (18), 160 (54), 132 (100), 105 (73), 51 (53); Anal. Calcd for $C_{16}H_{15}N_3O$: C = 72.43; H = 5.70; N = 15.84; O = 6.03; Found: C = 72.41; H = 5.68; N = 15.82; O = 6.01.

4.4.34. 2-(5,6-Dimethyl-1H-benzo[d][1,2,3]triazol-1-yl)-1-(4-methoxyphenyl) ethan-1-one (40)ssss

Solid: Yield: 67%; M.p.: 139–142 °C; ^{1}H NMR (300 MHz, DMSO-d_6), δ 8.13 (d, $J_{3',5'}$ = 8.7 Hz, 2H, H-2′, H-6′), 7.74 (s, 1H, H-2), 7.37 (s, 1H, H-1), 7.11 (d, $J_{2',6'}$ = 9.0 Hz, 2H, H-3′, H-5′), 6.26 (s, 2H, CH_2), 3.91 (s, 3H, OCH_3), 2.43 (s, 3H, H-1″, CH_3),2.41 (s, 3H, H-2″, CH_3); ^{13}C NMR (75 MHz, DMSO):δc 190.5, 163.9, 144.3, 137.1, 133.1, 133.0, 130.7, 127.0, 117.9, 114.1, 109.9, 55.6, 53.5, 20.9, 19.8; EI-MS *m/z* (% rel. abund.): 295 (M^+, 24), 267 (9), 239 (14), 160 (24), 135 (100), 105 (16); HREI-MS Calcd for $C_{17}H_{17}N_3O_2$ *m/z* 295.1321 Found: 295.1306; Anal. Calcd for: C = 59.10; H = 4.76; N = 15.20; O = 12.83; Found: C = 59.08; H = 4.75; N = 15.17; O = 12.81.

Acknowledgements

The authors are thankful to the Pakistan Academy of Sciences for providing financial support to Project No. (5-9/PAS/440).

References

[1] A. Chauhan, P.K. Sharma, P. Srivastava, N. Kumar, R. Dudhe, Plants having potential antidiabetic activity: a review, Der Pharm. Lett. 2 (3) (2010) 369–387.

[2] W.L. Li, H.C. Zheng, J. Bukuru, N. De Kimpe, Natural medicines used in the traditional Chinese medical system for therapy of diabetes mellitus, J. Ethnopharmacol. 92 (1) (2004) 1–21.

[3] N. Zaharudin, D. Staerk, L.O. Dragsted, Inhibition of α-glucosidase activity by selected edible seaweeds and fucoxanthin, Food Chem. 270 (2019) 481–486.

[4] M. Asgher, M.J. Asad, S.U. Rahman, R.L. Legge, A thermostable α-amylase from a moderately thermophilic Bacillus subtilis strain for starch processing, J. Food Eng. 79 (3) (2007) 950–955.

[5] A. Sundarram, T.P.K. Murthy, α-Amylase production and applications: a review, J. Appl. Environ. Microbiol. 2 (4) (2014) 166–175.

[6] M. Taha, M.T. Javid, S. Imran, M. Selvaraj, S. Chigurupati, H. Ullah, K.M. Khan, Synthesis and study of the α-amylase inhibitory potential of thiadiazole quinoline derivatives, Bioorg. Chem. 74 (2017) 179–186.

[7] M.D. Gunawan-Puteri, E. Kato, J. Kawabata, α-Amylase inhibitors from an Indonesian medicinal herb, *Phyllanthus urinaria*, J. Sci. Food Agric. 92 (3) (2012) 606–609.

[8] N. Jong-Anurakkun, M.R. Bhandari, J. Kawabata, α-Glucosidase inhibitors from Devil tree *(Alstonia scholaris)*, Food Chem. 103 (4) (2007) 1319–1323.

[9] U. Salar, K.M. Khan, S. Chigurupati, M. Taha, A. Wadood, S. Vijayabalan, S. Perveen, New hybrid hydrazinyl thiazole substituted chromones: as potential α-amylase inhibitors and radical (DPPH & ABTS) scavengers, Sci. Rep. 7 (1) (2017) 16980.

[10] G.S. Meneilly, E.A. Ryan, J. Radziuk, D.C. Lau, J.F. Yale, J.O.S.E. Morais, T. Wolever, Effect of acarbose on insulin sensitivity in elderly patients with diabetes, Diabetes Care 23 (8) (2000) 1162–1167.

[11] I. Kucukguzel, Ş.G. Kucukguzel, S. Rollas, G. Otuk-Sanış, O. Ozdemir, I. Bayrak, J.P. Stables, Synthesis of some 3-(arylalkylthio)-4-alkyl/aryl-5-(4-aminophenyl)-4*H*-1,2,4-triazole derivatives and their anticonvulsant activity, Il Farmaco 59 (11) (2004) 893–901.

[12] B.S. Holla, M. Mahalinga, M.S. Karthikeyan, B. Poojary, P.M. Akberali, N.S. Kumari, Synthesis, characterization and antimicrobial activity of some substituted 1,2,3-triazoles, Eur. J. Med. Chem. 40 (11) (2005) 1173–1178.

[13] Y.S. Sanghvi, B.K. Bhattacharya, G.D. Kini, S.S. Matsumoto, S.B. Larson, W.B. Jolley, G.R. Revankar, Growth inhibition and induction of cellular differentiation of human myeloid leukemia cells in culture by carbamoyl congeners of ribavirin, J. Med. Chem. 33 (1) (1990) 336–344.

[14] K.M. Khan, S. Siddiqui, M. Saleem, M. Taha, S.M. Saad, S. Perveen, M.I. Choudhary, Synthesis of triazole Schiff bases: novel inhibitors of nucleotide pyrophosphatase/phosphodiesterase-1, Bioorg. Med. Chem. 22 (22) (2014) 6509–6514.

[15] K. Sztanke, T. Tuzimski, J. Rzymowska, K. Pasternak, M. Kandefer-Szerszen, Synthesis, determination of the lipophilicity, anticancer and antimicrobial properties of some fused 1,2,4-triazole derivatives, Eur. J. Med. Chem. 43 (2) (2008) 404–419.

[16] M. Taha, M. Irshad, S. Imran, S. Chigurupati, M. Selvaraj, F. Rahim, K.M. Khan, Synthesis of piperazine sulfonamide analogs as diabetic-II inhibitors and their molecular docking study, Eur. J. Med. Chem. 141 (2017) 530–537.

[17] M. Taha, N.H. Ismail, S. Imran, M.H. Mohamad, A. Wadood, F. Rahim, K.M. Khan, Synthesis, α-glucosidase inhibitory, cytotoxicity and docking studies of 2-aryl-7-methylbenzimidazoles, Bioorg. Chem. 65 (2016) 100–109.

[18] M. Taha, S. Imran, N.H. Ismail, M. Selvaraj, F. Rahim, S. Chigurupati, S. Vijayabalan, Biology-oriented drug synthesis (BIODS) of 2-(2-methyl-5-nitro-1H-imidazole-1-yl) ethyl aryl ether derivatives, *in vitro* α-amylase inhibitory activity and *in silico* studies, Bioorg. Chem. 74 (2017) 1–9.

[19] U. Salar, K.M. Khan, M.I. Fakhri, S. Hussain, S. Tauseef, S. Ameer, S. Perveen, 1, 1'-Carbonyldiimidazole (CDI) mediated facile synthesis, structural characterization, antimicrobial activity, and *in silico* studies of coumarin-3-carboxamide derivatives, Med. Chem. 14 (1) (2018) 86–101.

[20] S. Yousuf, K.M. Khan, U. Salar, S. Chigurupati, M.T. Muhammad, A. Wadood, S. Perveen, 2′-Aryl and 4′-arylidene substituted pyrazolones: as potential α-amylase inhibitors, Eur. J. Med. Chem. 159 (2018) 47–58.

[21] M. Taha, N.H. Ismail, S. Lalani, M.Q. Fatmi, S. Siddiqui, K.M. Khan, M.I. Choudhary, Synthesis of novel inhibitors of α-glucosidase based on the benzothiazole skeleton containing benzohydrazide moiety and their molecular docking studies, Eur. J. Med. Chem. 92 (2015) 387–400.

[22] U. Salar, K.M. Khan, M. Taha, N.H. Ismail, B. Ali, S. Perveen, A. Wadood, Biology-oriented drug synthesis (BIODS): *In vitro* β-glucuronidase inhibitory and *in silico* studies on 2-(2-methyl-5-nitro-1*H*-imidazole-1-yl) ethyl aryl carboxylate derivatives, Eur. J. Med. Chem. 125 (2017) 1289–1299.

[23] F. Ali, K.M. Khan, U. Salar, M. Taha, N.H. Ismail, A. Wadood, S. Perveen, Hydrazinyl arylthiazole based pyridine scaffolds: synthesis, structural characterization, in vitro α-glucosidase inhibitory activity, and *in silico* studies, Eur. J. Med. Chem. 138 (2017) 255–272.

[24] M. Ramirez-Escudero, M. Gimeno-Perez, B. Gonzalez, D. Linde, Z. Merdzo, M. Fernandez-Lobato, J. Sanz-Aparicio, Structural analysis of β-fructo-furanosidase from *Xanthophyllomyces dendrorhous* reveals unique features and the crucial role of *N*-glycosylation in oligomerization and activity, J. Biol. Chem. 291 (13) (2016) 6843–6857.

[25] Molecular Operating Environment (MOE), 2016.08, Chemical Computing Group Inc., 1010 Sherbrooke St. West, Suite #910, Montreal, QC, Canada, H3A 2R7, 2016.

[26] E.P. Carreiro, P. Louro, G. Adriano, R.A. Guedes, N. Vannuchi, A.R. Costa, C.M.M. Antunes, R.C. Guedes, A.J. Burke, 3-Hydroxypyrrolidine and (3,4)-dihydroxypyrrolidine derivatives: inhibition of rat intestinal α-glucosidase, Bioorg. Chem. 54 (2014) 81–88.

[27] A.S. Singh, A.K. Agrahari, N. Mishra, M. Singh, V.K. Tiwari, An improved *N*-acylation of 1*H*-benzotriazole using 2,2′-dipyridyldisulfide and triphenylphosphine, Synthesis 51 (02) (2019) 470–476.

[28] W. Chen, R. Yan, D. Tang, S. Guo, X. Meng, B. Chen, Iodine-induced regioselective direct alkylation of azoles *via in situ* formed alkyliodide, Tetrahedron 68 (38) (2012) 7956–7959.

[29] A.R. Katritzky, Z. Luo, X.L. Cui, Synthesis of substituted piperidines from *N,N-bis*[(benzotriazol-1-yl) methyl] amines, J. Org. Chem. 64 (9) (1999) 3328–3331.

[30] D. Chang, D. Zhu, L. Shi, [3+2] Cycloadditions of azides with arynes *via* photolysis of phthaloyl peroxide derivatives, J. Org. Chem. 80 (11) (2015) 5928–5933.